Geochemistry, Geophysics, Geosystems®

AGU ADVANCING EARTH AND SPACE SCIENCE

RESEARCH ARTICLE
10.1029/2022GC010709

Key Points:

- Using olivine composition, we observe small-scale mantle heterogeneity resulted from the recycling of the different sediment compositions

Supporting Information:

Supporting Information may be found in the online version of this article.

Correspondence to:

D. Prelević and S. Conticelli,
dejan.prelevic@rgf.bg.ac.rs;
sandro.conticelli@unifi.it

Citation:

Günther, J., Prelević, D., Mertz, D. F., Rocholl, A., Mertz-Kraus, R., & Conticelli, S. (2023). Subduction-legacy and olivine monitoring for mantle-heterogeneities of the sources of ultrapotassic magmas: The Italian case study. *Geochemistry, Geophysics, Geosystems*, *24*, e2022GC010709. https://doi.org/10.1029/2022GC010709

Received 16 SEP 2022
Accepted 29 NOV 2022

Author Contributions:

Conceptualization: Jennifer Günther, Dejan Prelević
Data curation: Jennifer Günther, Dejan Prelević, Dieter F. Mertz, Alexander Rocholl, Regina Mertz-Kraus
Formal analysis: Alexander Rocholl, Regina Mertz-Kraus
Funding acquisition: Dejan Prelević
Investigation: Jennifer Günther, Dejan Prelević, Dieter F. Mertz, Sandro Conticelli
Methodology: Jennifer Günther, Dejan Prelević, Alexander Rocholl, Regina Mertz-Kraus
Project Administration: Dejan Prelević, Dieter F. Mertz
Resources: Jennifer Günther, Sandro Conticelli

Subduction-Legacy and Olivine Monitoring for Mantle-Heterogeneities of the Sources of Ultrapotassic Magmas: The Italian Case Study

Jennifer Günther[1], Dejan Prelević[1,2], Dieter F. Mertz[1], Alexander Rocholl[3], Regina Mertz-Kraus[1], and Sandro Conticelli[4,5]

[1]Institute for Geosciences, Johannes Gutenberg University, Mainz, Germany, [2]Faculty of Mining and Geology, Department of Petrology and Geochemistry, University of Belgrade, Belgrade, Serbia, [3]GeoForschungsZentrum Potsdam, Potsdam, Germany, [4]Dipartimento di Scienze della Terra, Università degli Studi di Firenze, Firenze, Italy, [5]Istituto di Geologia Ambientale e Geoingegneria, Consiglio Nazionale delle Ricerche, Roma, Italy

Abstract The origin of Italian kamafugites and lamproites is a matter of debate, not least due to their "crustal signature" displayed by trace element compositions and isotopic ratios, but also due to puzzling geodynamic significance. We combine in situ EMPA and LA-ICP-MS analyses with in situ analyses of oxygen isotopes (SIMS) on olivine from the Pleistocene San Venanzo kamafugites and Torre Alfina lamproites. Lamproitic olivine shows extremely high Mg# and Ni concentrations whereas Ca and Mn concentrations are low. Their $\delta^{18}O_{V\text{-}SMOW}$ values are very high up to +11.5 ‰. In kamafugites we recognize three genetically different olivine groups: (a) phenocrystic one with high Mg#, very low Ni, high Ca and Mn. Values of $\delta^{18}O_{V\text{-}SMOW}$ are up to +10.9 ‰; (b) melt-related xenocrystic grains that compositionally resemble lamproitic olivine; (c) skarn-related almost pure forsterite of extreme $\delta^{18}O_{V\text{-}SMOW}$ ~27 ‰, with negligible amounts of minor and trace elements. The melting and crystallization conditions of Italian kamafugites and lamproites indicate compositionally heterogeneous mantle sources on very small scales. Distinct geochemical features of the olivine macrocryst populations observed in kamafugite point to a range of processes occurring both within the magma storage and transport system. We suggest that the diversity of metasomatic agents was involved in mantle processes on local scales, coupled with magma mixing and/or the uptake of xenocrysts during magma ascend.

1. Introduction

By many measures, Italian Tertiary volcanic associations represent one of the most complex magmatism in the world. It reflects the response of the upper mantle to the convoluted, generally orogenic geodynamic evolution of this area (Peccerillo, 2005), which resulted in a considerable number of volcanic occurrences that fit textbook models neither for within-plate nor for arc environments. Most of the Oligocene to Quaternary volcanic associations, including arc-derived shoshonites and calc-alkaline suites, are generally characterized by universal enrichment of potassium coupled with invariably high incompatible trace element contents and isotopic composition approaching crustal values both in terms of concentration levels and fractionation (Conticelli, Guarnieri, et al., 2009). In more detail, two compositionally different ultrapotassic volcanic series are recognized: Si-undersaturated leucite-bearing with kamafugites as the most primitive lavas, and Si-saturated leucite-free (shoshonitic and high-K calk-alkaline) series including lamproites (Conticelli et al., 2010, 2015; Foley et al., 1987; Peccerillo, 2017). Importantly, the concurrent occurrence of the lavas from different series, even at single eruption centers (e.g., Boari, Tommasini, et al., 2009; Conticelli, Marchionni, et al., 2009; Conticelli et al., 2011, 2013; Perini & Conticelli, 2002), is another outstanding feature of the Italian volcanism, indicating heterogeneous mantle source(s) for the most primitive members of different magmatic series (Figure 1).

Despite a considerable number of studies, there has been still no consensus about two major aspects of the origin of this volcanism:

1. *The first issue* regards the geochemical signature, which usually compositionally overlaps upper continental crust composition, as demonstrated by enrichment in incompatible trace elements and potassium (Conticelli & Peccerillo, 1992). This has for a long time been a puzzling issue, especially for the lavas with the most extreme compositions like lamproites and kamafugites. Their geochemistry has often been used as magmatic

Supervision: Dejan Prelević, Dieter F. Mertz, Alexander Rocholl, Regina Mertz-Kraus, Sandro Conticelli
Validation: Jennifer Günther, Dieter F. Mertz, Alexander Rocholl, Regina Mertz-Kraus, Sandro Conticelli
Visualization: Jennifer Günther
Writing – original draft: Jennifer Günther, Dejan Prelević
Writing – review & editing: Dieter F. Mertz, Regina Mertz-Kraus, Sandro Conticelli

proxies to trace sediment recycling processes within the mantle, fingerprinted also in the more voluminous volcanics (e.g., Prelević et al., 2008). Alternatively to the mantle-related processes, many studies, especially ones focused on the origin of kamafugitic lavas (Iacono-Marziano et al., 2007, 2008) have proposed that their crustal geochemical signature, strong silica-undersaturation and extreme Ca-enrichment are due to the carbonate syntexis, that is, the assimilation of significant amounts of limestone by primitive potassic (shoshonitic) melts being able to produce leucititic/kamafugitic Si-undersaturated lavas (e.g., Peccerillo, 1998, 2005; Rittmann, 1933).

2. *The second issue* is the geodynamic model to be applied to complex tectonic settings, such as the Central Mediterranean. The most widely accepted is the *subduction model* that proposes active-margin processes, explaining extreme compositional variations of the Italian lavas and enrichment to be related to sediment recycling and formation of the metasomatic domains within the lithospheric mantle (Conticelli et al., 2015 and references therein). These domains are suggested to represent pyroxene-, phlogopite- and/or amphibole-rich lithologies occurring as veins or layers within peridotite (e.g., Ammannati et al., 2016 and references therein; Avanzinelli et al., 2020). According to this model, post-collisional changes in the thermal regime of the shallow mantle have triggered partial melting resulting in a range of primary melts variously enriched in potassium and calcium, and exceptionally variable Si-saturation (Ammannati et al., 2016). Primarily, this compositional range is explained to be the result of changes in the type of sediments recycled into the mantle sources of the magmas (carbonate-rich vs. pelitic), leading to a bifurcation between Si-undersaturated and Si-oversaturated lavas, and second, of gradually changing proportions of metasome-to surrounding mantle-melting (Ammannati et al., 2016; Avanzinelli et al., 2008; Conticelli, Guarnieri, et al., 2009, 2015). On the other hand, *the mantle-plume scenario* has gained attention in various versions denying widely accepted active-margin settings for Italian magmatism (e.g., Lavecchia & Stoppa, 1996; Lavecchia et al., 2006; Stoppa, 2003). The argumentation in favor of such geotectonic settings is diverse, for example, the occurrence of leucitites, carbonatites and kamafugites in Italy usually attributed to continental rift-related settings such as East Africa, as well as radiogenic isotope patterns universally suggested to represent plume compositions (e.g., Bell et al., 2004, 2005). Within that scope, the participation of sediments in magma genesis is usually confined to assimilation at shallow crustal levels (e.g., Boari, Tommasini, et al., 2009; Di Giuseppe et al., 2021; Peccerillo, 2017).

This study aims to evaluate different genetic models for the origin of ultrapotrassic lavas, kamafugites and lamproites, from the Mediterranean tectonic settings, taking the Italian samples as the most extreme compositions in terms of crustal-derived component enrichment. We focus here on the composition of olivine, which is the first crystallizing mineral phase in the majority of primitive mantle-derived melts. Olivine compositions have already been in use for constraining mantle sources and the presence of non-peridotitic metasomatic domains residing in the lithospheric mantle (e.g., Ammannati et al., 2016; Foley et al., 2013; Howarth & Harris, 2017) and thus is particularly suited for evaluating the potential role of subduction in the origin of the Italian lavas. Here we combine in situ major, minor and trace element measurements with in situ oxygen isotope analyses on igneous olivine macrocrysts and spinel inclusions hosted by the Pian di Celle kamafugite from San Venanzo and by the lamproite from Torre Alfina (Figure 1), both being archetypal and well-studied representatives of these types of ultrapotassic rocks. In situ analyses of oxygen isotopes within magmatic, earliest crystallizing mineral phases have the potential to make a valuable contribution to clarifying at which stage of petrogenesis the crustal signature dominantly affected the outstanding characteristic of the lavas. The in situ approach enables to resolve intragranular variations, and consequently, changes in physicochemical conditions during phenocryst crystallization. Especially in combination with in situ major and trace element analyses, the impact of processes at crustal levels might be distinguished from the genuine record of mantle conditions.

2. Geological Background

Beginning in the Miocene, the subduction of the Adriatic beneath the African plate induced the formation of the Apennines with the compressional front gradually moving eastward (Faccenna et al., 2004). The movement of the front was followed by magmatic activity migrating in the same direction. The magmatic activity commenced in the Corsica Magmatic Province during Miocene-Upper Pliocene times, then migrated eastward developing volcanism along the Tyrrhenian border of the Italian Peninsula in the Lower Pliocene (Conticelli et al., 2015). The volcanism in the intra-Apennines comprises a few small monogenetic centers of ultrapotassic pyroclastic rocks and minor lavas erupted on thick piles of about 5,000 to 6,000 m of Mesozoic limestones

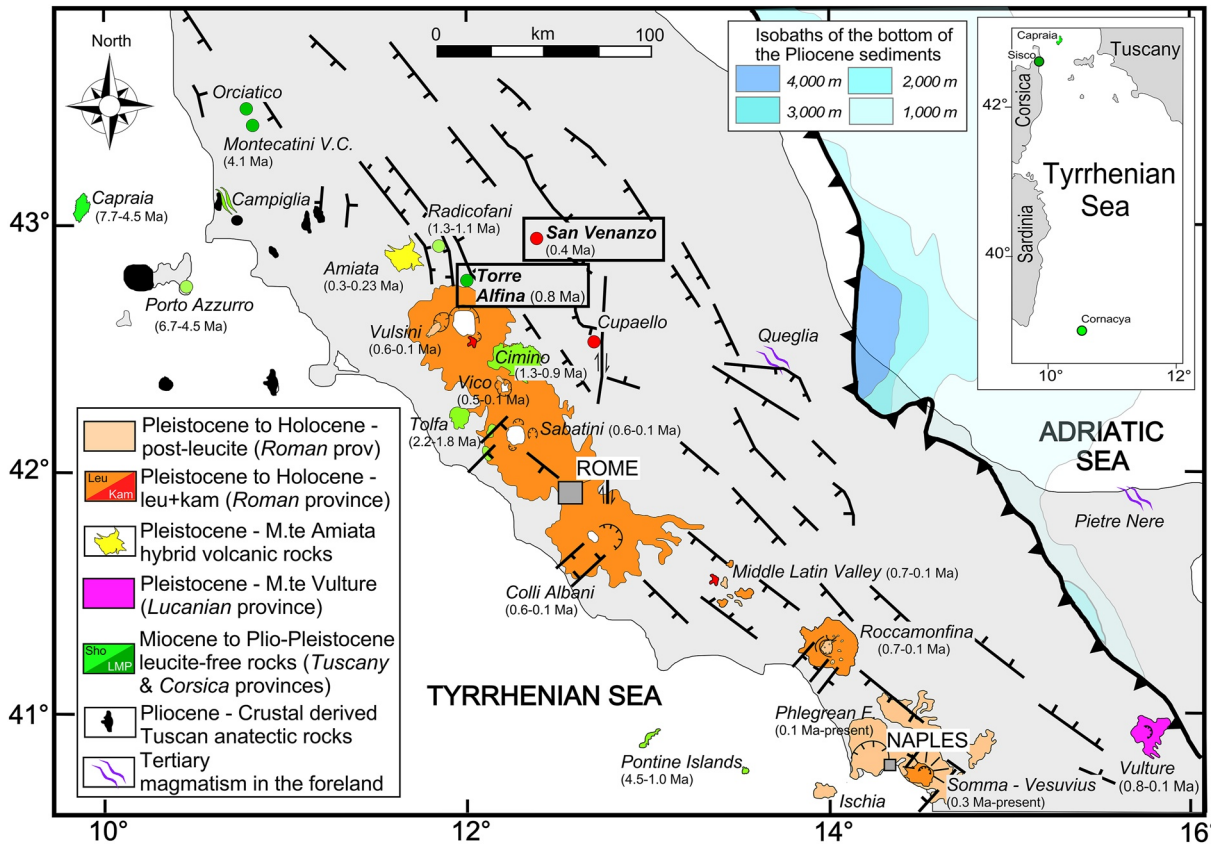

Figure 1. Distribution of ultrapotassic rocks in the Central Italian region revealing the sampling location (spots within the large rectangular shapes) and the distribution of the major magmatic provinces (events). Red spots and areas (kamafugites) and dark green spots (lamproites) mark the location sites of the most extreme endmembers of the orogenic magmatic activity. Modified after Conticelli et al. (2010, 2013, 2015).

overlain by Plio-Pleistocene continental sediments (Patacca et al., 2008). The magmatic activity was triggered by post-orogenic extensional tectonics and is recorded from the lower to middle Pleistocene (Conticelli et al., 2015 and references therein).

The majority of Italian lamproites belong to these igneous events. The Torre Alfina lavas is a typical representative of the Mediterranean type lamproites (Prelević et al., 2008) and is located in Central Italy about 150 km north of Rome (Figure 1). The small volcanic center, being active at around 0.82 Ma, is the source of a few lava flows and a volcanic neck. A more detailed description of the geological and volcanological setting is given by Conticelli (1998). Based on chemical and mineralogical composition, two types of lava can be distinguished as genetically linked by the assimilation of variable amounts of crustal rocks by the ascending magmas that are derived from the same source (Conticelli, 1998).

Italian kamafugites belong to the final event, namely the Roman Province, of the magmatism of Central Italy (Avanzinelli et al., 2009) in which silica-undersaturated magmas were produced during the Pleistocene parallel to the Apennine chain from Bolsena lake and San Venanzo to Vesuvius (Figure 1). Kamafugites are found in many cases intimately associated with the leucite-bearing lavas of the Roman Province volcanoes (e.g., Boari, Avanzineeli, et al., 2009; Boari, Tommasini, et al., 2009; Boari & Conticelli, 2007; Conticelli et al., 2010) and more rarely along the axial sector of the Apennine belt. The latter is claimed to belong either to the intra-Apennine Province (Peccerillo, 2017) or the Umbrian district of the Roman Province (Conticelli et al., 2015 and references therein).

Kamafugitic lavas were erupted at San Venanzo (Pian di Celle volcano) and Cupaello, whereas only the lavas at San Venanzo are olivine-phyric (Peccerillo, 2005 and references therein) (Figure 1). The mid-Pleistocene San Venanzo magmatic center consists of three small monogenetic volcanoes, namely San Venanzo, Pian di Celle and Celli being active at ca. 0.46 Ma (Stoppa, 1996; Zanon, 2005). They are characterized by the presence of

calcite-rich pyroclastic deposits, whereby at Pian di Celle two lava flows poured out (Zanon, 2005). The lavas represent the most mafic products of San Venanzo volcanic activity (Stoppa, 1996) and were sampled in this study.

3. Mineralogical and Geochemical Characterization of the Analyzed Samples

The studied samples are geochemically and mineralogically thoroughly characterized (Prelević & Foley, 2007; Prelević et al., 2008) and a comprehensive data set consisting of individual core-rim or core-mantle-rim olivine analyses can be found in Tables S1–S10 of the electronic appendix. In these data sets, the existing published data have been augmented with new extensive measurements, performed on well-characterized selected samples, and included a complete set of macro- and trace-elements as well as oxygen isotope measurements on the olivine grains.

The investigated samples from Torre Alfina (05TA01, 05TA02) belong to the lamproitic lavas least contaminated by crustal rocks. They consist of olivine as the only phenocrystic phase within a microcrystalline groundmass composed of olivine, phlogopite, clinopyroxene, sanidine, ilmenite and magnetite. Geochemically, the lava samples fit well within the range displayed by published data for Torre Alfina lamproite (Conticelli, 1998) showing high SiO_2 (55.0, 55.2 wt%) and MgO concentrations (7.42, 8.50 wt%), relatively low CaO (5.2, 5.3 wt%) and Al_2O_3 concentrations (12.5, 13.9 wt%) combined with very low Na_2O (0.9 wt%) and elevated K_2O concentrations (6.3, 7.4 wt%). According to Le Bas et al. (1986) the lavas are classified as olivine-latites. Rare Earth Element (REE) and mantle-normalized incompatible trace element patterns shown by the most primitive Torre Alfina lavas are fractionated and show the typical orogenic signature (Table S1). This is further supported by their high $^{87}Sr/^{86}Sr_i$ (0.71581–0.71589) and low $^{143}Nd/^{144}Nd_i$ values (0.51211–0.51212) as well as by Pb isotope ratios (e.g., $^{206}Pb/^{204}Pb = 18.67$; $^{207}Pb/^{204}Pb = 15.66$; $^{208}Pb/^{204}Pb = 38.85$) (Conticelli, 1998; Conticelli et al., 2002). Major and trace element analyses of olivine macrocrysts from Torre Alfina lamproite were published by Ammannati et al. (2016), Conticelli (1998), and Conticelli et al. (2015) as well as by Prelević et al. (2013). High Mg#, elevated Ni as well as low Ca concentrations and extraordinarily elevated Li contents were identified as typical features of the olivine phenocrysts. These host abundant Cr-spinel characterized by exceptionally high Cr#. Mantle olivine occurs as xenocrysts within the lamproite lavas.

The kamafugitic samples from Pian di Celle of San Venanzo volcanic center (05SV03, 05SV04) are classified as olivine melilitites, containing olivine macrocrysts (>100 μm) which are embedded in a holocrystalline groundmass of melilite, leucite, phlogopite, clinopyroxene, monticellite, kalsilite and calcite, whereas spinel, perovskite and apatite occur as accessory phases. The lavas are characterized by low SiO_2 (40.2, 41.7 wt%), high MgO (12.3, 12.6 wt%) and elevated CaO (13.5, 16.4 wt%) and K_2O (7.5, 7.8 wt%) concentrations along with moderate Na_2O contents (0.9, 1.2 wt%) (Table S1) and fit geochemically well into the range made up by published data for Pian di Celle lava (Conticelli et al., 2015 and references therein). Similar to Italian lamproites, REE and mantle-normalized incompatible trace element patterns for kamafugites also show a typical orogenic signature (Table S1). Initial values of $^{87}Sr/^{86}Sr$ (0.71027–0.71041), $^{143}Nd/^{144}Nd$ (0.512063–0.512080), $^{187}Os/^{188}Os$ (0.1888) as well as Pb isotope ratios ($^{206}Pb/^{204}Pb = 18.725$; $^{207}Pb/^{204}Pb = 15.648$; $^{208}Pb/^{204}Pb = 38.874$) (Conticelli et al., 2015 and references therein) show lower enrichment in comparison to lamproites. Oxygen isotope measurements of the bulk rock lava samples demonstrate $\delta^{18}O_{SMOW}$ values between +11 ‰ and +12 ‰ (Peccerillo, 2005 and references therein). Although existing data for olivine from Pian di Celle (Conticelli et al., 2015; Panina et al., 2003; Plechov et al., 2017) show a wide compositional variance, there is general agreement that high Mg#, low Ni and elevated Ca concentrations are the most prominent characteristics exhibited by phenocrystic olivine (Conticelli et al., 2015). In addition, a group of xenocrysts being almost pure forsterites containing negligible amounts of minor and trace elements is part of the mineral assemblage (Panina et al., 2003; Plechov et al., 2017). Their origin is proposed to be related either to a skarn or a contemporaneous carbonatitic melt.

4. Analytical Methods

Polished thin sections of whole rock lava samples 05SV03 and 05SV04 from Pian di Celle volcano were used to determine olivine major and minor element compositions by electron microprobe analysis (EMPA) and olivine minor and trace element concentrations by laser ablation-inductively coupled plasma-mass spectrometry

(LA-ICP-MS). For Torre Alfina lava samples 05TA01 and 05TA02, some major, minor and trace element analyses on olivine from polished thin sections, including a description of analytical methods, have been published by Prelević et al. (2013). These analyses are included in our data set (Table S2). In addition, major, minor and trace element analyses by EMPA and LA-ICP-MS as well as oxygen isotope measurements by secondary ion mass spectrometry (SIMS) were performed on olivine separates extracted from the four lava samples (Tables S1, S4, and S6).

For the preparation of the olivine separates, unaltered lava samples were crushed, washed, and sieved, and fresh olivine was handpicked under the binocular microscope. Olivine crystals of different grain sizes were mounted separately within a radius of 16 mm around the centers of the mounts. Within the center of each mount, a grain of San Carlos olivine (Pack & Herwartz, 2014) was placed, which served as reference material (RM) for SIMS oxygen isotope analyses. The grains were embedded in epoxy resin and polished to a roughness of less than 1 µm. Major and minor element compositions of olivine and olivine-hosted spinel inclusions from the thin sections and the olivine mounts were determined by EMPA (JEOL JXA 8200) at the University of Mainz. Operating conditions were 20 kV accelerating voltage, 20 nA beam current, 2 µm beam diameter and extended counting times on peaks (30 s for Si, 20 s for Fe and Mg, 50 s for Ni, Mn and Ca, 60 s for Cr and 160 s for Al). Synthetic and natural minerals were used as RMs for calibration. Intra-crystal variations were explored in rim-to-rim traverses; San Carlos olivine was analyzed as unknown. The accuracy and reproducibility of the analyses are the same as reported by Prelević et al. (2013).

Minor and trace element analyses of the mounted olivine separates and the olivine crystals within the thin sections were performed by LA-ICP-MS at the University of Mainz using an ESI NWR193 ArF excimer laser ablation system equipped with the TwoVol2 ablation cell, operating at 193 nm wavelength, coupled to an Agilent 7500ce quadrupole ICP-MS. Analyses were conducted with spot diameters between 40 and 50 µm, a repetition rate of 10 Hz and a fluence between 4 and 5 J/cm^2. Background intensities were measured for 15 s followed by 30 s of ablation and data collection on the sample and 20 s of wash out time. To account for instrumental drift, analyses on our samples of unknown composition were frequently bracketed by analyses of RMs for calibration and quality control. For olivine analyzed within the thin sections, raw data were processed using GLITTER 4.4.1 (Griffin et al., 2008). An in-house Excel Spreadsheet (Jochum et al., 2007), for which details of the calculations are given in Mischel et al. (2017), was used for processing data from the olivine mounts. In both cases, ^{29}Si was used as an internal standard applying for the samples the SiO_2 concentrations previously determined by EMPA and for the RMs applying the preferred values of the GeoReM database (http://georem.mpch-mainz.gwdg.de/, application version 18). When processing the raw data by GLITTER, NIST SRM 612 was using as calibration material and NIST SRM 610 when using Excel spreadsheet. Moreover, when using Excel spreadsheet, for Zn we used USGS BCR-2G as calibration material. Quality control materials (QCMs) used to monitor the accuracy and precision of the LA-ICP-MS analysis and calibration strategy were MongOL Sh11-2 (Batanova et al., 2019), USGS BCR-2G as well as NIST SRM 610 and 612 (when using either one for calibration). Element concentrations determined for the QCMs agreed mostly within 10% with the preferred values of the GeoReM database and had a precision of <10% (1RSD).

Oxygen isotope ratios ($\delta^{18}O_{V\text{-}SMOW}$) were determined using a Cameca 1280-HR SIMS at the GeoForschungsZentrum (GFZ), Potsdam. Samples were sputtered with a 10 kV Cs^+ primary beam of between 1.5 and 1.8 nA current and a spot size between 5 and 10 µm. A mass resolution of 1,600–1,700 at 10% peak height was attained. For charge compensation during analyses, a normal incidence electron gun was used. Ion intensities of ^{18}O and ^{16}O were measured in multi-collection mode by two off-axis Faraday cups. Analyses were run for 20 cycles of 4 s per cycle.

Analyses of samples of unknown composition were regularly bracketed by analyses of San Carlos olivine to check for a possible instrumental drift during analytical sessions. A linear parametrization as a function of time was used to cancel out this effect in the case of two analytical sessions where a small drift was observed (<0.15 ‰/h). Data were corrected for instrumental mass fractionation (IMF) by using San Carlos olivine ($\delta^{18}O_{V\text{-}SMOW}$ = 5.28 ‰, Pack & Herwartz, 2014) as RM. San Carlos olivine (Mg# = 91) shows Mg# well positioned within the range of Mg# made up by the samples (Mg# = 90–99). Matrix-dependent differences of IMF in the range of $Mg\#_{olivine}$ above 70 were shown to be negligible by previous studies (e.g., Bindemann, 2008; Gurenko et al., 2011) and thus we did not consider potential matrix effects. The repeatability of $\delta^{18}O$ analyses of San Carlos was better than 0.15 ‰ (1SD) for each session.

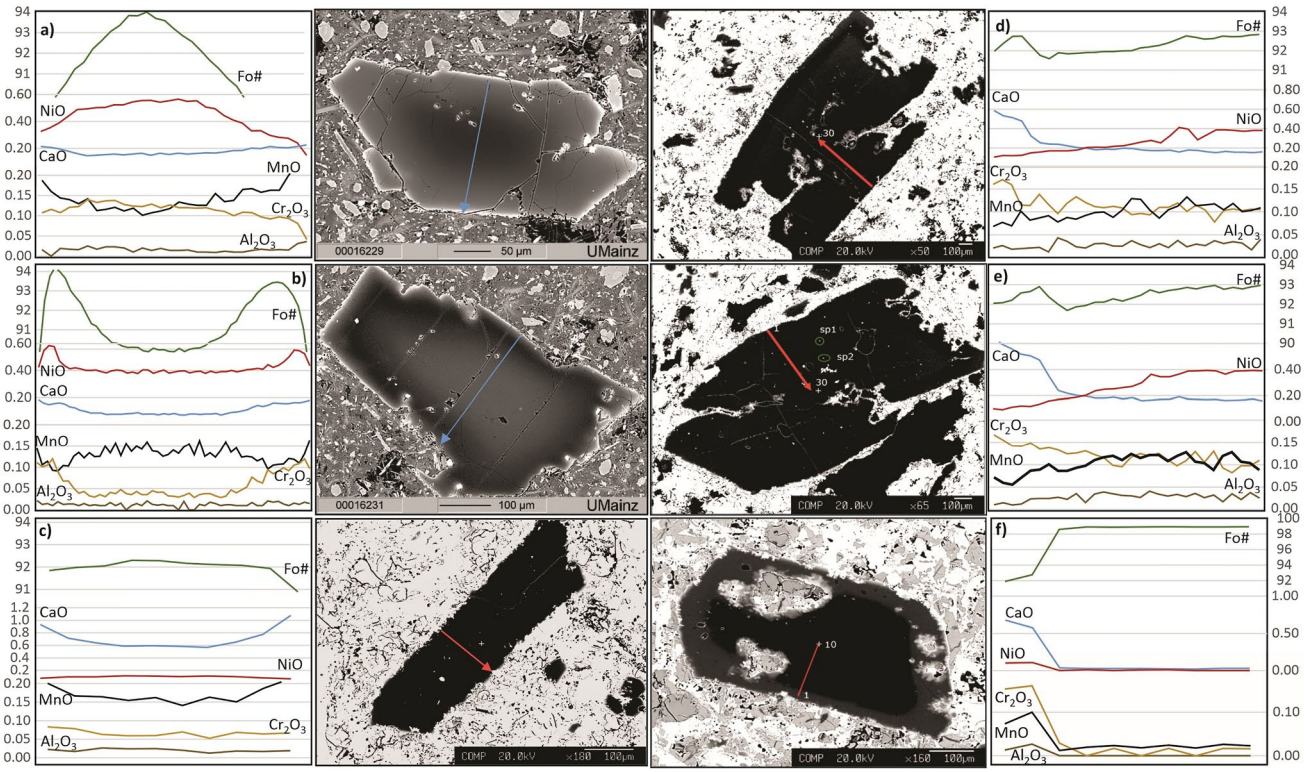

Figure 2. Representative backscattered electron images and line analyses (wt.%) by electron microprobe analyzer for (a) olivine phenocrysts from Tore Alfina lamproite; (b) mantle xenocrysts from Torre Alfina; (c) melt-related olivine phenocrysts from San Venanzo kamafugite; (d and e) melt-related olivine xenocrysts from San Venanzo kamafugite; (f) skarn-related olivine xenocrysts from San Venanzo kamafugite.

5. Results

A full data set including major, minor and trace element compositions as well as $\delta^{18}O$ of the olivine macrocrysts and major and minor element compositions of the spinel and sulphide inclusions are listed in the Tables S1–S10. All data from the data sets are plotted in Figures 2–8.

5.1. Olivine Macrocrysts From Torre Alfina Lamproite

The *olivine phenocrysts from Torre Alfina lamproite* are represented by euhedral to subhedral grains up to 400 µm in size and host abundant Cr-spinel inclusions (Figure 2a; Table S2). The results of major and minor element analyses obtained for the olivine macrocrysts from Torre Alfina lamproite are consistent with the ranges in elemental concentrations reported for Italian lamproites in general (Figures 2 and 3). Most forsteritic olivine compositions demonstrate a combination of exceptionally high Mg# and Ni concentrations, never observed in MORB-, OIB- and arc basalt-hosted olivine (Mg# up to 95.3; Ni up to 5,700 µg/g) (Figure 3a). Ca and Mn concentrations range from 510 to 1,620 and 420 to 1,590 µg/g, respectively (Figures 3b and 3c). The Ca concentrations are low compared to olivine from MORB but match those of some arc lava- and OIB-hosted olivine. Li concentrations in the olivine phenocrysts range from 20 to 24 µg/g (Figure 4). Similar high concentrations were reported for olivine from Mediterranean lamproites in general as well as from Italian leucitites (Ammannati et al., 2016; Prelević et al., 2013). In contrast, most MORB-hosted olivine shows average Li concentrations of 6.5 ± 0.3 µg/g (Gale et al., 2013), OIB-hosted olivine of <3 µg/g (Jeffcoate et al., 2007) and typical mantle olivine of <5 µg/g (Foley et al., 2013 and references therein). Concentrations of Zn vary between 50 and 60 µg/g and are comparable to reported concentrations for olivine from OIB (Foley et al., 2013), peridotites worldwide (Neumann et al., 2002; Rehfeldt et al., 2007, 2008) as well as from Mediterranean ultrapotassic lavas (Conticelli & Peccerillo, 1990; Prelević et al., 2013). Concentrations of Al are low and coupled with variable but relatively high Cr concentrations, overlapping worldwide lamproitic and kimberlitic olivine (Figure 4).

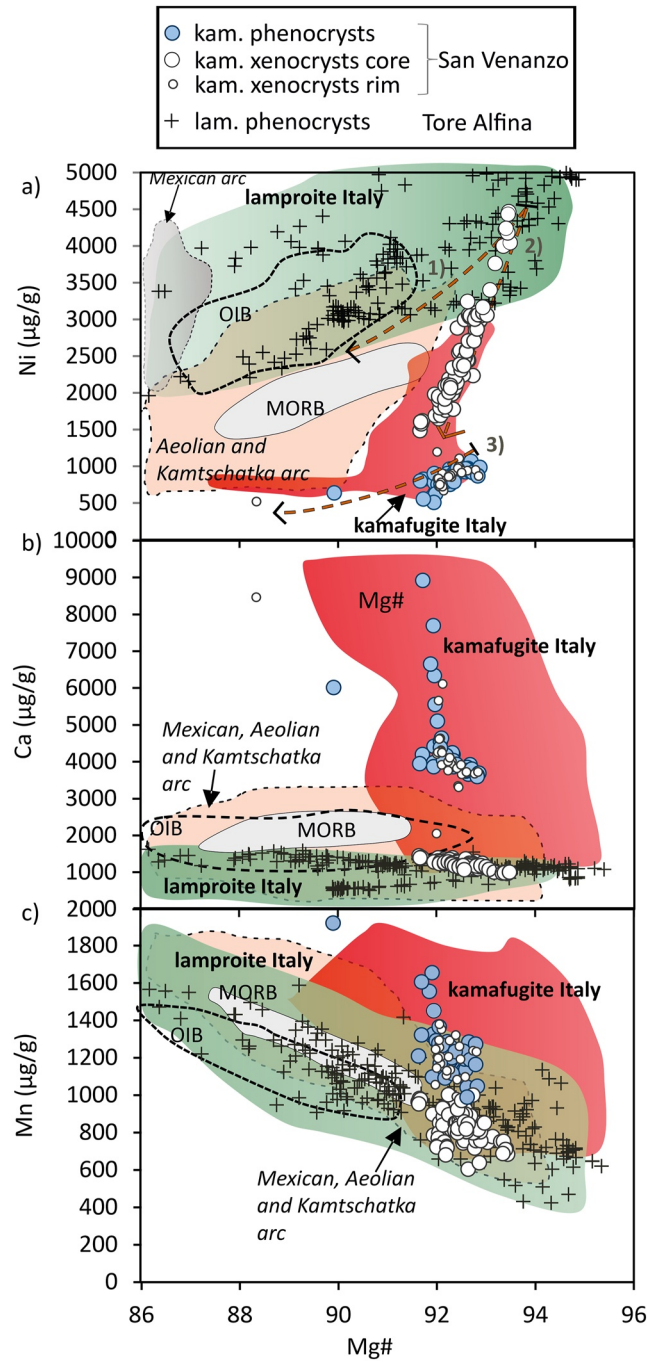

Figure 3. (a–c) Mg# versus Ni, Ca, and Mn in olivine macrocrysts from Pian di Celle kamafugite and Torre Alfina lamproite compared with olivine from OIB and MORB (Sobolev et al., 2005, 2007), Italian lamproites, leucitites, and kamafugites (Ammannati et al., 2016; Conticelli et al., 2015; Prelević et al., 2013), Mexican arc (Straub et al., 2008), Colli Albani Skarn (Di Rocco et al., 2012), Aeolian and Kamtschatka arc (GEOROC database; http://georoc.mpch-mainz.gwdg.de/georoc/: olivine from Aeolian and Kamchatka arc basalts; Query from 12 March 2019). Arrows (1 and 3) in diagram (a) indicate olivine compositional changes due to olivine + Cr spinel fractionation calculated by Petrolog3 software (Danyushevsky & Plechov, 2011) according to the model of Beattie (1993) at Ni-NiO—buffered conditions. (Arrow 2) indicates compositional changes due to olivine + Cr-spinel + Fe-Ni sulfide fractionation by combining equilibrium fractionation calculated by Petrolog3 with manual calculations (see Table S11 for details). The initial melt composition as starting point for calculations is an Italian lamproite (05RR01) from Prelević et al. (2013) for arrows (1 and 2), and whole rock data from this study (05SV04) for (arrow 3).

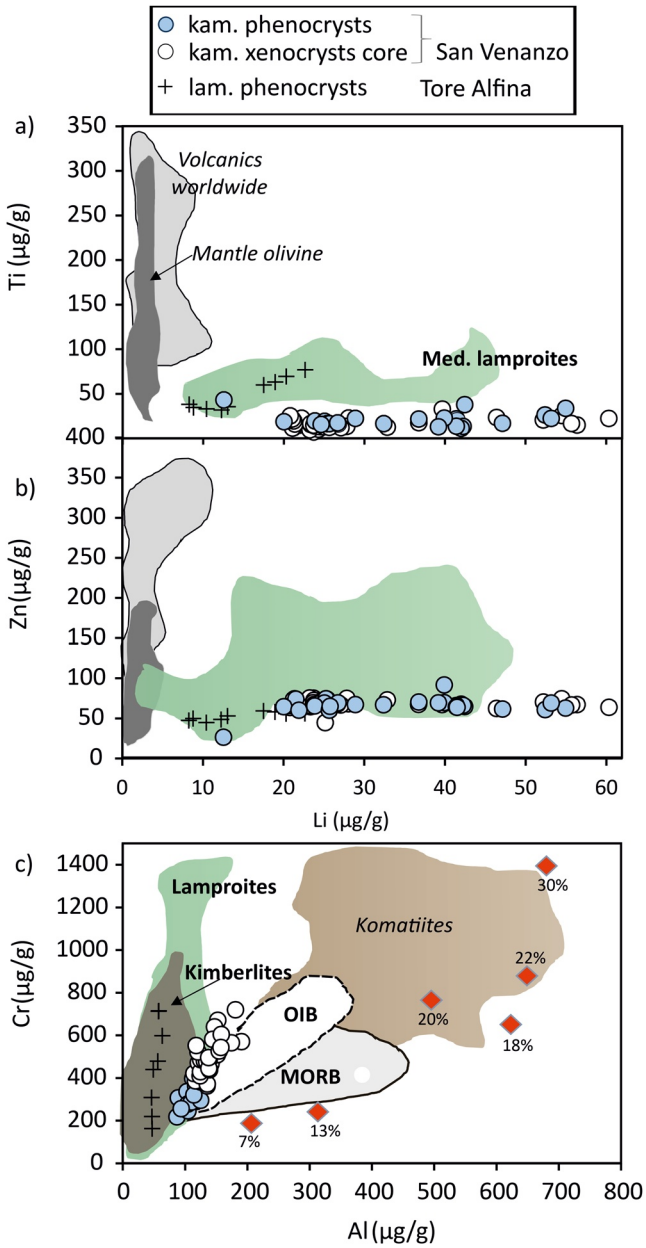

Figure 4. Trace element characteristics of the Tore Alfina and Pian di Celle olivine macrocrysts; (a and b) data sources: reference fields and data points for lamproite and leucitite olivine phenocrysts as in Figure 3. Li in typical mantle olivine from De Hoog et al. (2010); (c) Al versus Cr. Data for olivines from MORBs, OIBs and komatiites from Sobolev et al. (2005); lamproites and kimberlites from Prelević et al., 2013; red diamonds denote olivine compositions in equilibrium with experimental melts produced by different degrees of melting (Dasgupta et al., 2007; Hirose, 1997; Hirose & Kawamoto, 1995; Hirose & Kushiro, 1993). Data for Cr partitioning from GERM. We tentatively modeled olivine composition varying $Kd_{Al}^{Ol/liq}$ from 0.0006 to 0.004 for the increasing degree of melting between 1300 and 1500°C.

Besides phenocrystic olivine, in Torre Alfina lamproite we observed millimeter-sized *xenomorphic olivine mantle xenocrysts* typically showing reverse zoning, with core compositions having Mg# up to 91.5, NiO contents around 0.4 wt%, and CaO and Cr_2O_3 contents never exceeding 0.1 and 0.04 wt%, respectively (Figure 2b). Mantle xenocrysts are mantled by olivine of phenocrystic composition.

$\delta^{18}O_{V\text{-}SMOW}$ values from typical high-Fo, Ni-rich olivine phenocryst from Torre Alfina (Figure 5a) are invariably high from +11.4‰ to +11.5‰ and are to our knowledge the most elevated $\delta^{18}O$ values reported in fresh magmatic olivine. The $\delta^{18}O$ values are considerably higher compared to olivine hosted by *N*-type MORB (+4.9 ‰ to +5.3 ‰, Eiler, 2001), OIB (+4.6 ‰ to +6.1 ‰, Eiler, 2001; Genske et al., 2013), arc lavas (e.g., +4.9 ‰ to +5.8 ‰, Eiler et al., 2000) as well as compared to pristine mantle olivine (+5.2 ‰ ± 0.2 ‰, Mattey et al., 1994). On the other hand, mantle xenocrystic olivine from Torre Alfina lamproite demonstrates $\delta^{18}O_{V\text{-}SMOW}$ values similar to pristine mantle olivine (Table S8). One can speculate whether both olivine populations in Torre Alfina lamproites (phenocrysts and mantle xenocrysts) are derived from the same source, by analogy with a recent study of the large variability of $\delta^{18}O$ values between metasomatic phases and ambient peridotitic minerals observed in composite veined xenoliths from South-Eastern Spain. In those composite xenoliths, the $\delta^{18}O$ values range from +5.19 ‰, in peridotitic olivine, through +9.56 ‰ in orthopyroxene of the reaction rim of peridotite with the felsic vein, to +10.56 ‰ in plagioclase of the metasomatic vein (Avanzinelli et al., 2020; Dallai et al., 2019, 2022).

5.2. Olivine Macrocrysts From Pian di Celle Kamafugite (San Venanzo)

We observed two melt-related olivine populations in Pian di Celle kamafugite: *phenocrystic* and *xenocrystic* olivine. In addition, another, the most probably skarn-derived xenocrystic population has been observed (Figure 2) (see below).

The olivine *phenocrysts* are characterized by euhedral to subhedral grains not exceeding 500 µm in size and host abundant Cr-spinel inclusions (Figure 2c) (Table S2). The data plot into a more restricted range of low Ni and elevated Ca concentrations compared to the literature data pool. They show high Mg# (up to 92.8), Ca (up to 8,900 µg/g) and Mn concentrations (up to 1,900 µg/g) as well as low Ni (500–1,000 µg/g) contents in comparison to MORB-, OIB- and most arc basalt-hosted olivine (Figure 3). Notably, the most extreme Ca concentrations are shown by the outermost rims. Comparable to the lamproite phenocrysts, Li concentrations in kamafugite olivine phenocrysts range from 21 to 57 µg/g (Figure 4) and concentrations of Zn vary between 50 and 60 µg/g. The phenocrystic grains show $\delta^{18}O_{V\text{-}SMOW}$ values varying from +10.3 ‰ to +10.9 ‰ (Figure 5b). Thus, the kamafugite olivine phenocrysts show slightly lower values compared to the lamproite samples but are still extremely high relative to mantle- and olivine crystallized from typical basaltic lavas.

Xenocrystic, melt-related olivine population has not been previously described in the kamafugite lava from Pian di Celle. The substantially different elemental signature of the cores compared to the melt-related rims imply their xenocrystic origin (Figures 2d, 2e, and 3c; Table S7). In our sample collection, this group of olivine is most abundant and represented by subhedral, partially disintegrated grains ranging from ~500 µm to several millimeters in size (Table S7). It comprises high Mg# (up to 93.4) and Ni (up to 4,500 µg/g) cores that show a

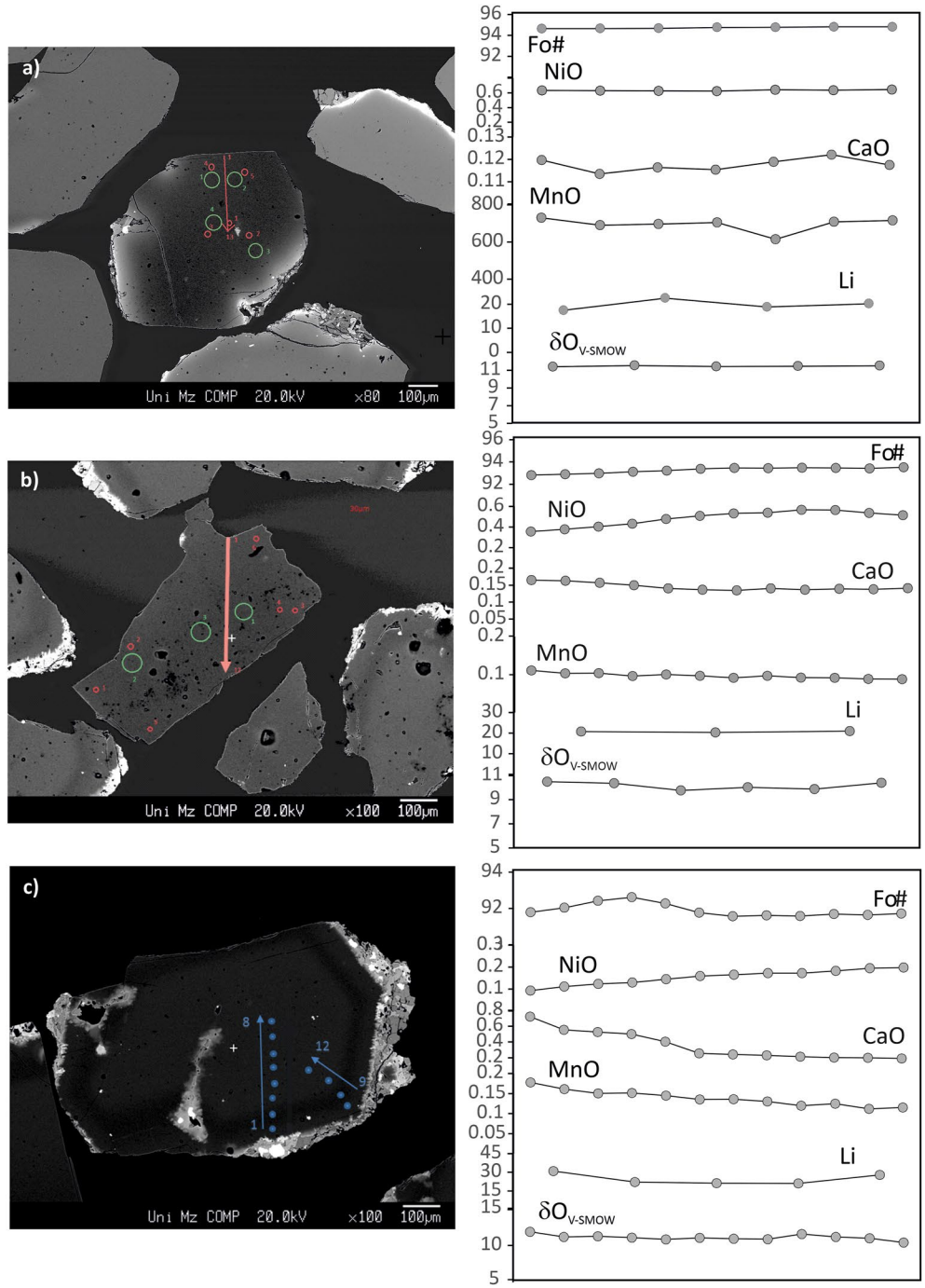

Figure 5. Line scan of Mg#, NiO, CaO, and MnO (in wt.%, by electron microprobe analysis), Li (in µg/g, by LAM-ICP-MS) and $\delta^{18}O_{V\text{-}SMOW}$ (in ‰, $^{18}O/^{16}O$ by analyses of oxygen isotopes) of representative olivine separates: (a) phenocrystic olivine from Tore Alfina lamproites; (b) olivine macrocrysts from San Venanzo kamafugites; (c) olivine xenocrysts from San Venanzo kamafugites. Please refer to Tables S7 and S8 for the explanation and numbering of the analyses.

slight rimward Mg# decrease coupled with an intense Ni decrease implying a very steep slope of Mg# versus Ni variation (Figure 3). Compositional features including Ca concentrations >1,000 µg/g, the zonation in Mg#, Ni and Ca as well as the lack of kink-bands and the presence of euhedral spinel inclusions, altogether indicate the unlikeliness of a mantle origin for these olivine cores. In addition to higher Ni, the cores display low Ca and Mn concentrations of 1,00–1,700 and 600–1,000 µg/g, respectively, which are also in contrast to the compositions of their rims and the olivine phenocrysts (Figure 3). The cores are mantled by olivine rims of 100–150 µm width

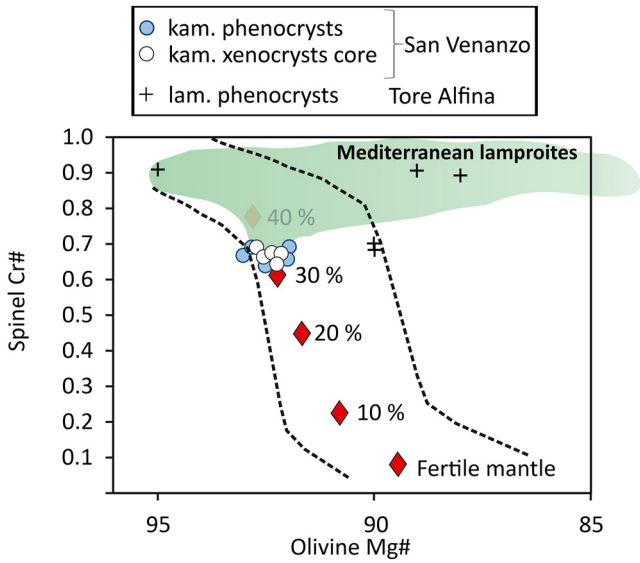

Figure 6. Olivine Mg# versus spinel Cr# illustrating the depleted character of the mantle sources of the melts that crystallized melt-related olivine from Tore Alfina lamproite and San Venanzo kamafugite. Red diamonds = olivine-spinel compositions of the peridotite that underwent former melt extraction to different extents (Arai, 1994). The dashed line is the „olivine-spinel mantle array" (OSMA) after Arai (1994). Reference fields were redrawn from Prelević and Foley (2007).

with higher Mg#, higher Ca and lower Ni concentrations that compositionally match the phenocrystic olivine crystals (Table S2). In terms of Mg# and Ni as well as Ca and Mn concentrations, the xenocrystic olivine cores show a significant resemblance with olivine hosted by Italian lamproites including Torre Alfina lamproite (Figure 2). When we compare the kamafugitic xenocrystic olivine with the Torre Alfina olivine, the sole difference is represented by the slope in the plot Ni versus Mg# (Figure 3a). Such a sudden drop in Ni concentration is different when compared with the usual Mg# versus Ni variation in for example, lamproites or more voluminous lavas like MORBs and OIBs caused by simple olivine (±Cpx) fractionation (Figure 3), and in our view has considerable genetic significance (see below). Therefore, we modeled different mineral assemblages as being produced along the liquid line of descent to simulate this unusually steep positive linear trend. The result of modeling suggests that the coprecipitation of olivine, Cr-spinel and Fe-Ni sulphide represents the best fit (see figure caption and Table S11 for the details of modeling).

Similar to the phenocrystic groups of olivine of Torre Alfina and Pian di Celle, the xenocrystic olivine cores show substantially elevated Li concentrations between 23 and 58 µg/g, and $\delta^{18}O_{V\text{-}SMOW}$ values between +9.2 ‰ and +10.8 ‰ (23 analyses on 3 grains) (Figures 4 and 5b). Besides, Zn concentrations of 77–96 µg/g lie in a similar range compared to the lamproite and kamafugite phenocrysts. The transition from the core to the rim zone is indicated by an abrupt increase in Mg# and Ca as well as a smooth decrease in Ni and an increase in Mn concentrations.

Skarn-derived, xenocrystic olivine population is subordinate comprising anhedral to subhedral, partially disintegrated grains smaller than 500 µm (Figure 2f). They show compositional plateaus of extremely high Mg# between 97 and 99.5. Olivine of such high Mg# is very rare and known from skarn and exoskarn from Colli Albani volcanic district (Di Rocco et al., 2012) and Vulture carbonatite (Rosatelli et al., 2000). The high Mg# is accompanied by unusually low concentrations of all minor and trace elements (Figures 2 and 3). For example, Ca concentrations vary between 170 and 400 µg/g, Mn concentrations between 100 and 190 µg/g and Ni concentrations are <30 µg/g. Cores are rounded and mantled by olivine of phenocrystic composition. They are Cr-spinel-free with inclusions only observed in the rims. $\delta^{18}O_{V\text{-}SMOW}$ values of these olivine grains show a limited range varying around +27 ‰ (Table S7) and are substantially higher relative to other olivine populations.

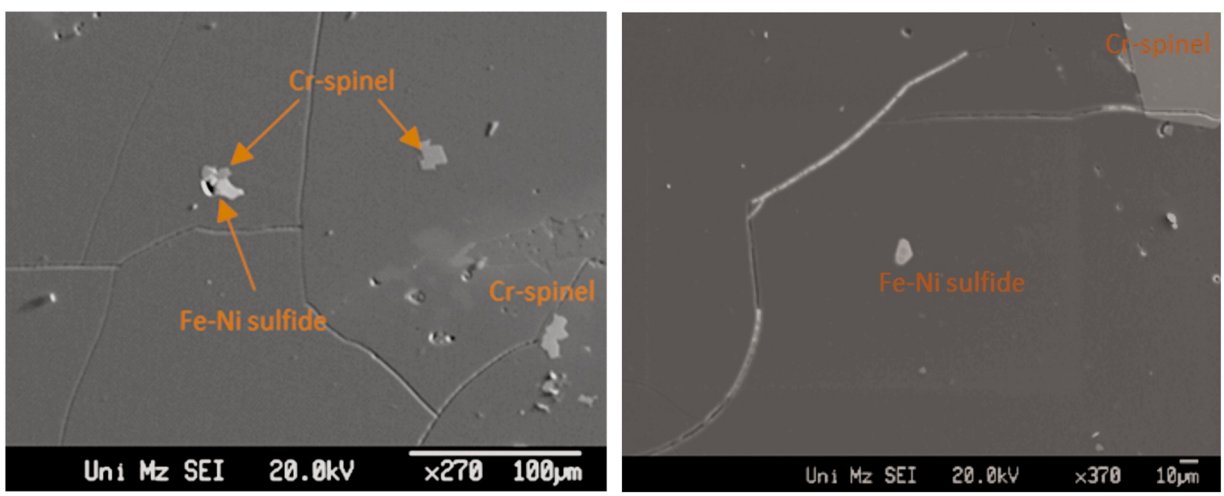

Figure 7. Ni-Fe-Cu sulphide grains in xenocrystic olivine from San Venanzo kamafugite.

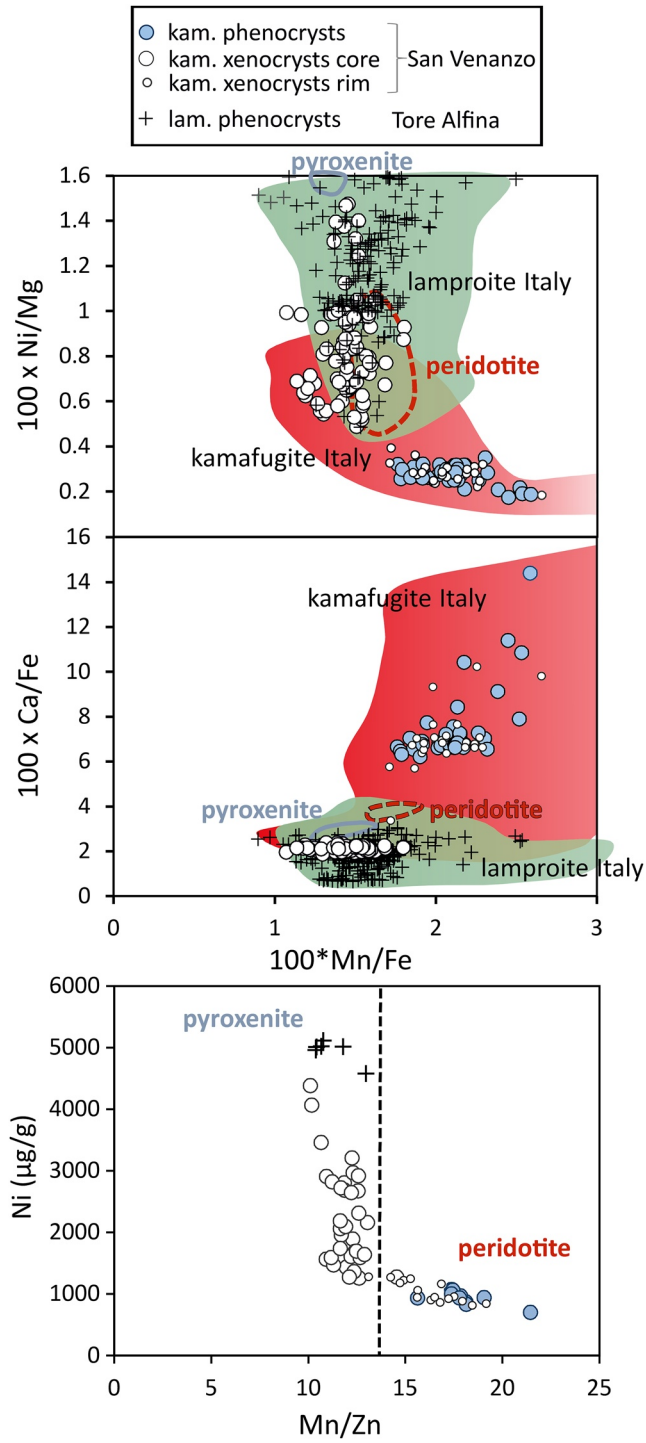

Figure 8. Geochemical indicators in olivine illustrating the role of different mantle mineralogies (peridotite vs. pyroxenite) in the origin of Pian di Celle kamafugite. Data sources: (a and b) Pyroxenite and peridotite reference fields redrawn after Sobolev et al. (2007), the data source for lamproite-, leucitite- and kamafugite-hosted olivine and Torre Alfina lamproitic olivine same as in Figure 3a; (c) reference fields for olivine crystallized from peridotite- and pyroxenite-derived melts redrawn after Howarth and Harris (2017), data sources for lamproite and leucitite olivine phenocrysts same as in (a); (d) dashed line separating pyroxenite-versus peridotite-derived host melts after Howarth and Harris (2017), data sources for lamproite and leucitite olivines same as in (a).

5.3. Spinel and Sulphide Inclusions in Lamproites and Kamafugites

Euhedral to subhedral spinel inclusions from Torre Alfina and Pian di Celle olivine pheno- and xenocrysts show a moderate compositional difference (Table S7), with lamproitic spinels having slightly higher Cr# and Mg# (Figure 6). They are Cr-spinels characterized by elevated Cr# (0.64–0.90), high Mg# (62–87) and $Fe^{3+}/\sum Fe$ of 0.24–0.47.

Olivine xenocrysts from Pian di Celle kamafugites host Fe-Ni sulphides (Figure 7; Table S9), with Co and Cu occurring as trace elements, SO_2 concentrations vary between 30 and 37 wt%, FeO between 30 and 59 wt% and NiO between 3 and 33 wt%. The data on the Fe-Ni sulphides reveal a negative correlation between FeO and NiO most probably induced by the progressive crystallization of olivine along with Fe-Ni sulphide and spinel.

6. Discussion

The composition of olivine from the studied ultrapotassic lavas is controlled by the nature of the source regions, conditions and proportions of partial melting, and the degree of modification from source to surface. Based on steadily decreasing Fo-contents, all analyzed olivine grains are inferred to reflect at least some degree of melt modification by fractionation (Figure 3). On the other hand, the presence of xenocrystic olivine populations represents strong evidence that their parental magmas interacted with geochemically distinct crystal mushes potentially derived from a different magmatic source and the mantle itself.

Our data support earlier observations that lamproitic olivine (Torre Alfina) is extremely forsteritic, demonstrating exceptionally high Li and Ni, and low Ca concentrations. It hosts spinel inclusions of extraordinarily elevated Cr#. Similarly, we also confirm that the phenocrystic olivine population from the kamafugitic lavas (San Venanzo) share high Mg# values and Li concentrations as well as spinel inclusions of elevated Cr# with the lamproitic ones, but demonstrate substantial differences in terms of Ni and Ca contents. There are also many significant differences illustrated in Figures 2–8 when plotting several parameters including Mn/Zn, Ca/Fe and Ni. On the other hand, among the populations of melt-related olivine recognised in the kamafugitic lavas, the primitive xenocrystic cores fully resemble the compositional features observed in lamproitic olivine. Importantly, all investigated melt-related olivine grains from both lava types have extraordinally high $\delta^{18}O$ values, similar to the values observed in heavily metasomatized composite mantle xenoliths originating through metasomatism with crust-derived melts (e.g., Avanzinelli et al., 2020; Dallai et al., 2019, 2022).

Our observations of olivine textures and geochemistry augmented with the new oxygen isotope data and the previous geochemical data on the same rocks are below used to discuss the petrogenesis and evolution of the most extreme ultrapotassic lavas of the Italian volcanism. After discussing the significance of olivine as a general petrogenetic monitor, we concentrate on the following issues that emerge from our study:

1. Does the ultimate origin of the geochemical signature demonstrated by kamafugitic lavas and their olivine phenocrysts result after the assimilation of bedrock limestone by the mantle-derived alkaline magmas on its way to the surface, or does it represent a genuine mantle fingerprint ultimately originating from its contamination by sedimentary material during active margin processes?
2. What is the origin of the xenocrystic olivine cargo observed in the kamafugite? If we consider that they originated from previous lamproitic crystal mushes and cumulates disturbed during kamafugitic magma ascent, what is the most viable model for the coeval occurrence of these extreme ultrapotassic lava types?
3. Do the Ni-sulphides observed in the xenocrystic olivine from kamafugites have caused the steep slope on the bivariate diagram of Mg versus Ni, and what is their significance?

Finally, we address the issue of subduction-induced sediment recycling, the melt transfer and interaction with the lithosphere below the alkaline magmatic centers. In a comprehensive view, the unique synergy of the above processes including also the integration of multiple batches of variably differentiated mantle-derived melts will be crucial for the compositional evolution of these extremely alkaline melts and their crystal cargo.

6.1. Olivine as a Petrogenetic Monitor

A wide application of olivine in delineating and interpreting many petrogenetic processes is driven by its very simple composition. Because of the straightforward link between Mg# in olivine and its host melt, this parameter

is widely used to identify primitive mantle-derived melts and the degree of fractionation experienced by magmas (Falloon et al., 2007; Putirka, 2005; Putirka et al., 2007), although not fully applicable to ultracalcic melts (Lustrino et al., 2022). A number of minor- (Ni, Mn, Ca, and Cr), trace-elements (Ti, Li, Zn, Al, Co, P, V, and Sc) as well as oxygen and lithium isotopic compositions, have been in use as geochemical tracers that have recently gained significant attention as mantle metasome monitors (e.g., Ammannati et al., 2016; Foley et al., 2013; Howarth & Harris, 2017).

Coupled with spinel composition, Mg# of olivine may constrain the extent of mantle partial melting and mantle depletion (e.g., Arai, 1994). The amount of partial melting simultaneously influences the compositions of both spinel and olivine: in natural peridotites, the modal proportion of clinopyroxene gradually decreases and finally disappears in the course of partial melting, which is followed by an increase in the Cr# of spinel and Mg# of olivine. This should also be reflected in the olivine and spinel pairs newly crystallizing from a primary melt because the composition of the liquidus phases should be close to that of residual phases in the mantle source (Yoder & Tilley, 1962). However, the bulk chemistry of the system changes once the magma is separated from its source, and therefore, it must be considered that the temperature, pressure, oxygen fugacity and the degree of partial melting may affect their chemistry and so confuse the proxy signal.

Olivine minor element compositions may indicate the presence of non-peridotitic source lithologies. The concentrations of Ni, Ca, and Mn as well as Ni/Mg, Ca/Fe, and Mn/Fe in olivine were applied for estimating the mineralogical nature of the mantle sources of some Hawaiian OIB lavas (Sobolev et al., 2007). Olivine-poor pyroxenitic mantle lithologies show a lower bulk mineral/melt distribution coefficient (D) for Ni compared to peridotitic sources, whereas Ds for Ca and Mn are higher. Moreover, olivine is the only mantle mineral displaying a higher D for Fe than for Mn. For that reason, pyroxenite-derived melts and their olivine crystals should be higher in Ni, Ni/Mg and lower in Mn, Mn/Fe, Ca, and Ca/Fe (Foley et al., 2013; Sobolev et al., 2007).

Besides Ni, Ca, Mn and Fe, some other first-row transition elements as Co and Zn and ratios like Zn/Fe, Mn/Zn and Ni/Co are suitable as tracers for the mineralogical composition of mantle residua (e.g., Howarth & Harris, 2017; Le Roux et al., 2010), as these ratios do not fractionate during magmatic processes. Conversely, they will be fractionated differently by partial melting of peridotite than by pyroxenite. Thus, pyroxenite-derived melts and their olivine phenocrysts are suggested to display higher Mn/Zn, Zn/Fe, and Ni/Co compared to those derived from peridotitic source lithologies.

Olivine compositions can help to trace the process of subduction-induced sediment recycling into the mantle inducing transformation from peridotite to olivine-free pyroxenite assemblages. Sediment recycling will cause a rise in Li concentrations in the mantle sources and melt-related olivine phenocrysts (Conticelli et al., 2015; Foley et al., 2013; Prelević et al., 2013), as Li is strongly enriched in the continental crust compared to the mantle. Moreover, the oxygen isotope signature recorded in olivine can track crustal recycling. Large areas of the upper mantle are considered homogenous concerning oxygen isotope compositions with the average bulk mantle of $+5.5 \pm 0.2$ ‰ $\delta^{18}O_{SMOW}$ (Mattey et al., 1994). Crustal materials show deviating $\delta^{18}O$ toward more positive values in the case of continental crust and variable but often more negative values in the case of altered oceanic crust meaning that oxygen isotope ratios in igneous olivine phenocrysts represent a highly effective tool able to discriminate and quantify genetically different geochemical components. In addition, the examination of the compositional zonation together with isotopic compositions may be used to distinguish olivines crystallized from magmas originating from the heterogeneous mantle containing a sediment component, from olivines derived from intracrustal igneous sources affected by assimilation of crust and/or mixing with silicic melts of different isotopic compositions (Bindeman, 2008).

Thus, oxygen isotope ratios in igneous olivine phenocrysts may indicate mantle metasomatism in the source rocks and provide information on the general type of subducted crust acting as a source for metasomatic agents (e.g., Gurenko & Chaussidon, 2002; Kokfelt et al., 2006; Thirlwall et al., 2004). Particularly in combination with olivine minor and trace element compositions, $\delta^{18}O$ allows a more detailed specification of the nature of recycled materials.

6.2. Fingerprinting Metasomatically Modified Mantle Source of Lamproites

Lamproites have some of the most extreme geochemical compositions among mantle-derived melts (e.g., Mitchell & Bergman, 1991 and references therein). Their orogenic counterparts are characterized by high K_2O contents

(3–12 wt%), enrichment of K_2O relative to Na_2O with $K_2O/Na_2O >> 2$ at MgO > 3 wt%, crust-like trace element pattern and Sr, Nd, and Pb isotopic compositions (Foley & Peccerillo, 1992; Prelević et al., 2008 and references therein). The Mediterranean orogenic lamproitic rocks are generated by the melting of so-called metasomes that represent metasomatic assemblages originating during subduction-induced sediment/crust recycling and melting in the mantle (vein + wall rock model of Foley, 1992). The metasomes are a result of the extreme melt-mantle reaction, probably generated during the Alpine and Apennine subduction, which severely enriched the mantle peridotite in phlogopite and pyroxene transforming variously depleted lithospheric peridotite into mixed domains consisting of fertile olivine-free phlogopite-pyroxenites within peridotite (e.g., Conticelli et al., 2015; Lustrino et al., 2011; Prelević et al., 2008). The usual recurrence of ultrapotassic magmatism in the Mediterranean (Sokol et al., 2020) implies that the recycling of the crustal component(s) does not necessarily have to result in volcanism, but just produces these metasomes that may melt during later tectonomagmatic trigger, as being recently experimentally confirmed (Förster et al., 2019).

Studied Italian lamproites resemble their Mediterranean counterparts in terms of all geochemical signals typical for the continental crust. An ultimate indication for the recycling of crust-derived sediments in the mantle source of the melts from which their olivine has crystallized is provided by elevated olivine $\delta^{18}O$ and Li values. Figure 5 demonstrates that the $\delta^{18}O$ values of phenocrystic olivine are consistently above +11 ‰, independent of the transition from cores to phenocrystic rims as indicated by the change in the Fo# component. Thus, the oxygen isotope ratios in lamproitic olivine are considered genuine records of the mantle source without significant low-pressure crustal contamination. This modification is most probably attributed to the Oligocene to Holocene (Molli, 2008 and references therein) subduction of the Adriatic plate beneath the Apennines as oxygen isotope data suggest that metasomatic enrichment and partial melting processes in the mantle have to be nearly contemporaneous. Otherwise, the high $\delta^{18}O$ signature within mantle metasomes would not be preserved because reequilibration with the surrounding mantle is a relatively fast process at high temperatures assumed to occur on a few million-year timescales (Dallai et al., 2019 and references therein).

Extremely high Fo olivine phenocrysts and their high-Cr spinel inclusions are a common feature of Mediterranean lamproites (Prelević et al., 2013) and kamafugites (Conticelli et al., 2004; Stoppa & Cundari, 1998), which has been observed also in our study. The extent of fractionation and the effects of pressure, temperature and oxygen fugacity cannot be responsible for the exceptionally high Mg# in olivine and Cr# in spinel inclusions. For example, the extreme fractionation and/or very low oxygen fugacity may explain high Cr# in spinel, but cannot simultaneously drive highly forsteritic olivine composition, simply because they will cause the opposite effects (e.g., Hill & Roeder, 1974). Moreover, a universal depletion of Al (and Ca in lamproites) in all liquidus minerals (phlogopite, clinopyroxene, olivine itself, see Figure 3) is observed (Conticelli & Peccerillo, 1992), which collectively point to harzburgitic mantle source component. Therefore, most studies agree that the mantle source of kamafugites and lamproites must be ultra-depleted.

Enrichment in Ni and high-Mg# signature as well as the Cr-rich spinel inclusions demonstrated by Italian lamproitic olivines further discount shallow crustal contamination as being responsible for the highly positive oxygen isotope signature. Given the above discussion, these features imply crystallization from a primitive mantle-derived melt and indicate an initially harzburgitic mantle source (Figure 6). Their consistently high-Ni and low-Ca signature (Figure 8) may be explained by the low D_{bulk} for Ni between pyroxenite and melt, whereas the low Ca concentrations are suggested to reflect a low quantity of clinopyroxene in the melting assemblage of their source (Förster et al., 2019). Plots of Ni/Mg and Ca/Fe versus 100 * Mn/Fe as well as of Ni versus Mn/Zn, 10,000 * Zn/Fe versus 100 * Mn/Fe, and Ni/Co > 20 further confirm the pyroxenitic nature of the mantle source of the melts crystallizing the lamproitic olivine crystals (Figure 8).

In summary, the results obtained by olivine $\delta^{18}O$ in addition to elemental analyses suggest that subduction-induced sediment recycling produced high $\delta^{18}O$ pyroxenite mantle domains serving as a source for the lamproite-type melts that crystallized olivine of this very specific geochemical signature.

6.3. Kamafugitic Olivine Phenocrysts: Mantle Versus Intracrustal Processes

Highly positive $\delta^{18}O$, high Li and Ca as well as low Ni concentrations coupled with their high Mg# are outstanding compositional features of the kamafugitic olivine phenocrysts. Two viable models may explain the origin of these grains and the $\delta^{18}O$ data represent decisive parameter to discriminate between them:

1. Carbonate syntexis including the assimilation of significant amounts of limestone by primitive potassic melts (e.g., Rittmann, 1933);
2. Mantle metasomatism driven by the recycling of carbonate-rich sediments (Ammannati et al., 2016).

(1) Carbonate syntexis including the assimilation of significant amounts of limestone by primitive potassic melts (e.g., Rittmann, 1933) was proposed to produce leucititic/kamafugitic low-Ni/high-Ca (Di Stefano et al., 2018) and high-Fo olivine (Lustrino et al., 2022) crystallizing from Si-undersaturated melts. Such olivine was experimentally generated after doping a primitive basaltic magma (Mg# ~ 78) with up to 20 wt% of $CaCO_3$ at various temperatures (e.g., Di Stefano et al., 2018; Lustrino et al., 2022). In this scenario, the olivine crystals would be related to the early stages of carbonate syntexis during magma ascent to the surface, when a high-T, olivine-saturated magma is contaminated by a large amount of Ca-rich melts from the skarn shell.

Our new oxygen isotope data demonstrate that the carbonate syntexis scenario would be hardly applicable to explain the origin of the kamafugite phenocrysts; if the parental melt would be strongly to moderately SiO_2-undersaturated nephelinite or basanite with a "regular" mantle oxygen isotope signature ($\delta^{18}O$ values around +5.2 ‰), simple modeling demonstrates that the assimilation of large portions of limestone of 24–30 vol% is required for a melt to drive the $\delta^{18}O$ values toward equilibrium with the olivine crystals (Table S12). The assimilation of limestone in this order of magnitude would freeze the whole system and would have a significant impact on physicochemical conditions during the crystallization of the phenocrysts and spinel inclusions. As a result, for example, spinel would show Al-enrichment and Cr-depletion (e.g., Gaeta et al., 2009; Wenzell et al., 2001, 2002), whereas olivine should be considerably enriched in Ca (Iacono-Marziano et al., 2007, 2008) with more than 2.5% of CaO (Lustrino et al., 2022). Moreover, it would never result in potassium enrichment as observed in kamafugites. Alternatively, the carbonate syntexis scenario in which the parental magma has a composition similar to the lamproite could theoretically lead to kamafugitic melt that can crystallize olivines resembling those found in the lavas. However, given the oxygen isotope composition of lamproitic olivine ($\delta^{18}O$ values $\geq$ +11 ‰), as well as the values for limestone ($\delta^{18}O$ values > +20 ‰; Turi, 1970), this assimilation would lead to an increase in $\delta^{18}O$, which is not observed; quite opposite, kamafugitic olivine has $\delta^{18}O$ < +10 ‰.

(2) The kamafugite phenocrysts and lamproite-like olivine xenocrysts share similarly elevated $\delta^{18}O$ values and Li concentrations, unequivocally indicating a genetic kinship through the involvement of the sedimentary component(s). Mantle metasomatism driven by the recycling of carbonate-rich sediments represents the most plausible interpretation for the origin of kamafugitic olivine phenocrysts. This is already indicated by the highly elevated Ca and Li concentrations as well as $\delta^{18}O$ values in the olivine crystals. Moreover, the presence of clinopyroxene in the source is suggested by relatively high Zn/Fe values that were shown to be sensitive to residual clinopyroxene during mantle partial melting (Le Roux et al., 2010). Figures 8a–8c show that the kamafugite phenocrysts have elevated 100 * Mn/Fe and Mn/Zn and plot along the olivine-bearing (peridotite) melting trend in 100 * Mn/Fe versus 10,000 * Zn/Fe and Ni versus Mn/Zn diagrams. In addition, Ni/Co < 10 (Table S4) suggests that olivine also plays a considerable role in the mantle residuum. Thus, data on the phenocrystic olivine may indicate that a phlogopite-wehrlitic lithology dominates the mantle source assemblage of the kamafugitic melts, which is also in accordance with the model proposed earlier (Ammannati et al., 2016). They proposed a two-stage model in which the first stage demands the production of these phlogopite-wehrlite metasomes and CO_2 at pressures ≥2 GPa generated by the recycling of subducted carbonate-rich sediments into the depleted mantle (e.g., Grassi & Schmidt, 2011; Poli, 2015), and during the second stage, metasome melting produces proto-kamafugitic primary melts with low Ni and high Ca concentrations. In this case, the substantial Ni depletion and Ca enrichment in the olivine is a consequence of an increase or decrease of the Ni or Ca bulk partition.

In summary, it is suggested that the geochemical signature of the kamafugite olivine phenocrysts represents a genuine mantle fingerprint ultimately originating from a high $\delta^{18}O$ lithospheric mantle contaminated by sedimentary material. As stated in Section 6.2, the time span between mantle metasomatism and partial mantle melting has to be relatively short implying metasomatism has taken place in the course of the Apennine subduction. Mantle contamination and limited limestone assimilation are two processes not necessarily mutually exclusive (Iacono-Marziano et al., 2007, 2008; Lustrino et al., 2020); the assimilation of certain quantities of bedrock

limestone by the kamafugite magmas in the last stages of their evolution is suggested by the presence of resorbed rims showing an increase in Ca concentrations demonstrated by all olivine grains (e.g., Figure 4).

6.4. Kamafugitic Xenocrysts: Olivine Crystallized From the Lamproitic Melt That Underwent Ni-Sulfide Fractionation

The distinct geochemical features of the olivine macrocryst populations from San Venanzo are indicative of a range of processes occurring both within the magma storage and transport system and in the mantle source. Figures 2–7 show that the xenocrystic olivine demonstrates all highly specific geochemical fingerprints characteristic of lamproitic olivine, including high Fo content, exceptionally high Li and Ni, low Ca concentrations, elevated Cr# in spinel inclusions and high $\delta^{18}O$ averaging +11 ‰. This means that the crystal cargo observed in the kamafugite, besides phenocrysts that grew in the magma itself, includes xenocrysts from previous, unrelated lamproitic magma. This implies entrainment from previous lamproitic crystal mushes and cumulates disturbed during kamafugitic magma ascent with remobilization of these crystals by the recharge magma pulses and new rims growth around pre-existing ones. Figure 7 demonstrates that the $\delta^{18}O$ values are consistently high, independent of the transition from cores to phenocrystic rims, which is indicated by the rise in Fe and a decrease in Mg concentrations. Since Fe and Mg are elements with a considerably faster diffusion rate than oxygen (Chakraborty, 2010 and references therein), the oxygen isotope system is considerably less prone to disturbances caused by abrupt changes in the melt composition. This means that the high $\delta^{18}O$ of the xenocrystic olivine cannot be potentially explained by the diffusion of oxygen from the surrounding melt that has been hypothetically contaminated by the continental crust during the intrusion.

The exceptional *nickel variation of the lamproitic xenocrysts in kamafugite,* illustrated by the steep slope on the bivariate diagram of Mg versus Ni, represents a single difference when compared with the variation demonstrated by olivine from lamproites (Figure 3). We link this variation with the presence of Fe-Ni sulphides hosted by the cores of lamproitic xenocrysts (Figure 7). This is also supported by quantitative models that compare the fractionation of different mineral assemblages and its impact on the variation of Mg and Ni (Figure 3a). Our geochemical modeling requires coprecipitation of ~80 (wt.)% olivine and 20% Ni-sulphide to explain the data, implying that the steep slope of the positive correlation seen in Figure 3a cannot be a result of the fractionation of olivine plus Cr spinel only and must be additionally controlled by fractionation of some Ni-bearing phase, for example, Ni sulfide observed as inclusions. Their presence (Figure 7) implies that the primary lamproitic mantle-derived melt was sulfide saturated indicating that a small-volume sulfide melt separated during the early stages of the evolution of this melt. Sharygin et al. (2003) reported the occurrence of magmatic Ni-rich sulfide inclusions in Ni-rich olivine phenocrysts from Smokey Butte and Leucite Hills lamproites and proposed the high-Ni signature probably being characteristic of the mantle sources of lamproites. According to Barnes et al. (2013) Ni-rich sulfides form particularly in olivine-saturated Ni-rich magmas. The presence of Ni-sulfide inclusions in olivine xenocrysts in kamafugites (Table S9) in which Ni is preferentially incorporated, may explain the observed sudden drop of olivine Ni concentrations for a relatively narrow range of Mg# (Figure 3a).

An important question arises from the above discussion: what triggers early sulfide saturation at nominally oxidizing conditions related to the crustal recycling within the active margin system that produced lamproitic melt? Carbon and sulfur species dominantly control fluid-mediated redox reactions in the mantle, thereby indirectly controlling the level of sulfur saturation. If we assume that the parental melt of mantle-derived orogenic volcanism crystallized olivine at oxidizing conditions similar to QFM + 1—QFM + 4, the amount of sulfur needed to attain sulfide saturation would be between 0.2 and 1.4 wt.%. Nevertheless, the sulfide saturation will take place at considerably lower concentrations at more reducing conditions (Jugo, 2009) which are proposed for lamproitic melt formation. Namely, most experimental (Foley, 1985) and empirical studies (Prelević et al., 2005) of lamproites suggest very reducing conditions from QFM −3 log units $fO2$, down to equilibration at the MW buffer. For example, the subduction of pelitic sediments rich in organic matter is likely to provide the sulfur-bearing species into the mantle wedge overlying the subducted slab and therewith enrich mantle domains in sulfur. Thus, partial mantle melts might carry considerable amounts of this component. Moreover, the abundance of Ni in melts is known to decrease the sulfide saturation surface considerably (Ariskin et al., 2013; Smythe et al., 2017) and as lamproitic olivines are suggested to originate from a melt rich in Ni, early sulfide saturation seems probable.

The presence of sulfide melt separated during the early stages of the evolution of the lamproitic melt may be indirectly indicated by their Mo depletion and very high $\delta^{98/95}$Mo, the highest recorded so far in the orogenic settings (Casalini et al., 2019) and require an isotopically heavy sedimentary component recycled in their mantle source. The Mo fractionation depends on redox conditions, and we speculate that pelitic sediments rich in organic matter subducted and reacted with the mantle, which induced the enrichment of organogenic S, reducing the mantle source of lamproites.

7. A Snapshot of a Shift From Pelitic to Carbonate-Rich Sediment Flux Recycled Within the Mantle Below the Apennines

In the orogens like the Alpine-Himalayan belt, sediment recycling within the mantle wedge contributes considerably to the geochemistry of arc magmas but also generates metasomatic domains within the lithospheric mantle that may be activated during or even after active-margin processes have ceased, that is, in the course of subsequent post-collisional magmatism (e.g., Hole, 1988; Prelević et al., 2013; Sokol et al., 2020). Carbonates and silicates are compositional end-member constituents of the sediment load in the subducting column, and their recycling represents a principal source of fluids and/or melts derived from the subducting crust that will metasomatize the overriding mantle. Metasomatic agents are represented by hydrous silicate melts (Green & Ringwood, 1968), aqueous fluids (Tatsumi & Kogiso, 1997) and supercritical siliceous, carbonatitic, and alkaline solutions (Kessel et al., 2005; Massonne, 1992; Scambelluri & Philippot, 2001; Thomsen & Schmidt, 2008). The metasomatic effects of the recycling of silicate- and carbonate-rich sediments on the mantle-wedge will be contrasting because of different melt compositions. The melting of siliciclastic sediments will produce granitic/rhyolitic melt (Sekine & Wyllie, 1982; Wyllie & Sekine, 1982) and its interaction with the peridotitic mantle will result in silica and potassium enrichment and depletion in HFSEs relative to LILE situated within a universally present phlogopite clinopyroxenites (Förster et al., 2019, 2020). On the other hand, with the increase of carbonate component in the siliciclastic sediments, it is expected that its melting will result in the melt of granitic composition at lower pressures (2.5 GPa), and of phonolitic composition at higher pressure (5.0 GPa) (Thomsen & Schmidt, 2008). At a higher temperature, the conjugate carbonatitic melt will form with alkaline granitic to phonolitic melts. In both cases, the mantle peridotite should be refertilised with dolomite-phlogopite wehrlites.

The story of the generation of broadly coeval kamafugites and lamproites in San Venanzo is one of the heterogeneous mantle source in an extensive, trans-crustal magmatic system. Magma mixing and sulfide saturation are prominent processes and are associated with episodic emplacement of magmas into the shallow crust, but do not drive the overall chemical evolution of magmas. In the following, we will present our working model that explains a geodynamic scenario in which the coincidence of the most extreme representative of Si-undersaturated and Si-oversaturated magmas could have taken place (Figure 9).

The melting of siliciclastic pelitic sediments and the interaction of this melt with the peridotitic mantle will universally result in the crystalization of phlogopite-clinopyroxenite metasomes (Förster et al., 2019, 2020). The melting of these metasomes has produced lamproitic melts, which we anticipate has happened in Torre Alfina 0.8 Ma, but also broadly simultaneously in the San Venanzo without known surface appearances (Figure 9). With the increased carbonate component in the siliciclastic sediments approaching the melting region in the slab, the resulting melt interacting with the mantle will form dolomite-bearing phlogopite wehrlites. These metasomes produced kamafugite slightly later 0.4 Ma. The kamafugitic parental magmas interacted with previously cumulated crystal mushes resulting in the presence of abundant xenocrystic olivine populations.

The geochemical transition from Si-saturated lamproitic, to Si-undersaturated kamafugitic orogenic magmas, strongly points to major changes in the composition of the subducting material beneath the Apennine active margin close to the Miocene–Pliocene boundary (Figure 9). The variability in geochemical signatures recognized in olivine hosted by the Pian di Celle kamafugite may be considered a unique snapshot of the "moment" of this transition. It mirrors mineralogical heterogeneities in the lithospheric mantle below the Apennines which has been significantly modified by subduction-induced continental sediment recycling. This modification is attributed to the Oligocene to Holocene (Molli, 2008 and references therein) subduction of the Adriatic plate beneath the Apennines (Figure 9).

The phenocrystic population of olivine from San Venanzo kamafugite reflects a depleted mantle source metasomatically modified by melts of carbonate-rich sediments that were introduced into the sub-arc mantle via

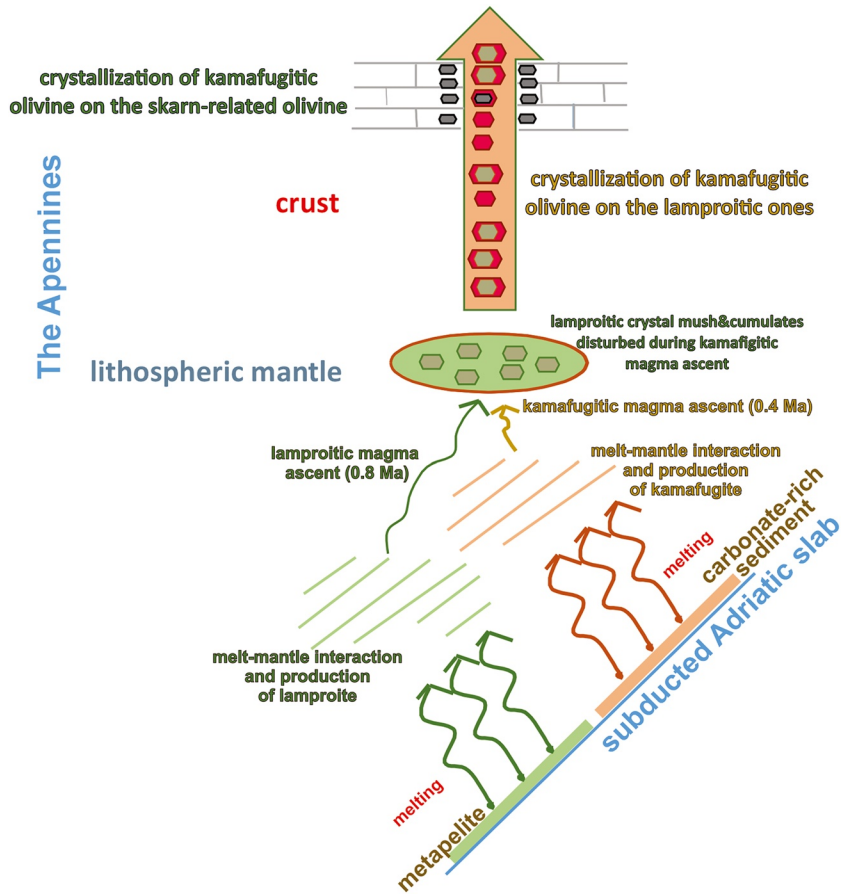

Figure 9. Illustration of the proposed model for the formation of the Pian di Celle kamafugite lavas and hosted olivine. The geochemical transition from Si-saturated lamproitic, to Si-undersaturated kamafugitic orogenic magmas has been generated due to major changes in the composition of the crustal material comprising Adriatic plate subducting beneath the Apennine active margin. For a further explanation see the text.

subduction (Figure 9). Mineralogically, the mantle metasome may be classified as phlogopite-wehrlite. The melt-related olivine xenocrysts display a primitive mantle-derived signature also suggesting an initially depleted mantle source metasomatically modified by SiO_2-rich alkaline partial melts of subducted pelitic sediments (Figure 9). Thus, crystallization of the xenocrystic cores from a lamproite-type melt derived from an olivine-poor orthopyroxene-dominant mantle source is implied (e.g., Ammannati et al., 2016). Like the bimodal character of the Italian orogenic magmatism (Roman vs. Tuscan Magmatic Province) in general, the coexistence of kamafugite and lamproite phenocrystic olivine crystals within one single lava represents the compositional diversity of sediments (carbonate-rich vs. pelitic) recycled into the sub-arc mantle, however, on laterally small scales. These multiple subduction imprints observed in one lava are not a unique feature to Pian di Celle but have for example, also been described for Latera volcano located about 40 km SW of San Venanzo (Nikogosian et al., 2016).

The heterogeneity of the kamafugite magma in terms of olivine composition is related to the diversity of metasomatic agents involved in mantle processes on local scales. Various mechanisms such as magma mixing and/or the uptake of xenocrysts during magma ascend may be responsible for the joint presence of different olivine types. The uptake of primitive, melt-related xenocrysts into mafic magmas appears to be a common phenomenon and is suggested to dominate over the formation of phenocrysts, especially in subduction-related, volatile-rich settings (e.g., Zellmer et al., 2013, 2014). This is in accordance with the observed supremacy of the xenocrystic over the phenocrystic olivine crystals, indicating this process might be prevalent.

Data Availability Statement

The complete data sets produced during this study is available at Figshare with a DOI https://doi.org/10.6084/m9.figshare.21651269.

Acknowledgments
The authors gratefully appreciate the help of Nora Groschopf and Dr. Stephan Buhre during analyses by EMPA. Uwe Dittmann made a valuable contribution by preparing most olivine mounts for SIMS analyses. The content-related comments by Vladica Cvetković were of great benefit in the final stages of manuscript preparation. The research was funded by the German Research Foundation (DFG; project PR 1072/9-1), the Italian Ministry of University and Research (COFIN; projects # 20158A9CBM and 20224T2JF4) and by the Science Fund of the Republic of Serbia through project RECON TETHYS (7744807).

References

Ammannati, E., Jacob, D., Avanzinelli, R., Foley, S. F., & Conticelli, S. (2016). Low Ni olivine in silica-undersaturated ultrapotassic igneous rocks as evidence for carbonate metasomatism in the mantle. *Earth and Planetary Science Letters*, *444*, 64–74. https://doi.org/10.1016/j.epsl.2016.03.039

Arai, S. (1994). Characterization of spinel peridotites by olivine-spinel compositional relationships: Review and interpretation. *Chemical Geology*, *113*(3–4), 191–204. https://doi.org/10.1016/0009-2541(94)90066-3

Ariskin, A. A., Danyushevsky, L. V., Bychkov, K. A., McNeill, A. W., Barmina, G. S., & Nikolaev, G. S. (2013). Modeling solubility of Fe-Ni sulfides in basaltic magmas: The effect of nickel. *Economic Geology*, *108*(8), 1983–2003. https://doi.org/10.2113/econgeo.108.8.1983

Avanzinelli, R., Bianchini, G., Tiepolo, M., Jasim, A., Natali, C., Braschi, E., et al. (2020). Subduction-related hybridization of the lithospheric mantle revealed by trace element and Sr-Nd-Pb isotopic data in composite xenoliths from Tallante (Betic Cordillera, Spain). *Lithos*, *352–353*, 105316. https://doi.org/10.1016/j.lithos.2019.105316

Avanzinelli, R., Elliott, T., Tommasini, S., & Conticelli, S. (2008). Constraints on the genesis of the potassium-rich Italian volcanic rocks from U/Th disequilibrium. *Journal of Petrology*, *49*(2), 195–223. https://doi.org/10.1093/petrology/egm076

Avanzinelli, R., Lustrino, M., Mattei, M., Melluso, L., & Conticelli, S. (2009). Potassic and ultrapotassic magmatism in the circum-Tyrrhenian region: Significance of carbonated pelitic vs. pelitic sediment recycling at destructive plate margin. *Lithos*, *113*(1–2), 213–227. https://doi.org/10.1016/j.lithos.2009.03.029

Barnes, S. J., Godel, B., Gürer, D., Brenan, J. M., Robertson, J., & Paterson, D. (2013). Sulfide-olivine Fe-Ni exchange and the origin of anomalously Ni-rich magmatic sulfides. *Economic Geology*, *108*(8), 1971–1982. https://doi.org/10.2113/econgeo.108.8.1971

Batanova, V. G., Thompson, J. M., Danyushevsky, L. V., Portnyagin, M. V., Garbe-Schönberg, D., Hauri, E., et al. (2019). New olivine reference material for in situ microanalysis. *Geostandards and Geoanalytical Research*, *43*(3), 453–473. https://doi.org/10.1111/ggr.12266

Beattie, P. (1993). Uranium-thorium disequilibria and partitioning on melting of garnet peridotite. *Nature*, *363*(6424), 63–65. https://doi.org/10.1038/363063a0

Bell, K., Castorina, F., Lavecchia, G., Rosatelli, G., & Stoppa, F. (2004). Is there a mantle plume below Italy? *Eos, Transactions American Geophysical Union*, *85*(50), 541. https://doi.org/10.1029/2004EO500002

Bell, K., Lavecchia, G., & Stoppa, F. (2005). Reasoning and beliefs about Italian geodynamics. *Bollettino della Societa Geologica Italiana*, *5*, 119–127.

Bindemann, I. (2008). Oxygen isotopes in mantle and crustal magmas as revealed by single crystal analysis. *Reviews in Mineralogy and Geochemistry*, *69*(1), 445–478. https://doi.org/10.2138/rmg.2008.69.12

Boari, E., Avanzinelli, R., Melluso, L., Giordano, G., Mattei, M., De Benedetti, A., et al. (2009). Isotope geochemistry (Sr-Nd-Pb) of leucite-bearing volcanic rocks from 'Colli Albani' volcano, Roman Magmatic Province, Central Italy: Inferences on volcano evolution and magma genesis. *Bulletin of Volcanology*, *71*(9), 977–1005. https://doi.org/10.1007/s00445-009-0278-6

Boari, E., & Conticelli, S. (2007). Mineralogy and petrology of Mg-rich calc-alkalic, potassic, and ultrapotassic associated rocks: The middle Latin valley monogenetic volcanoes, Roman Magmatic Province, Southern Italy. *The Canadian Mineralogist*, *45*(6), 1443–1469. https://doi.org/10.3749/canmin.45.6.1443

Boari, E., Tommasini, S., Laurenzi, M. A., & Conticelli, S. (2009). Transition from ultrapotassic kamafugitic to sub-alkaline magmas: Sr, Nd, and Pb isotope, trace element and ^{40}Ar-^{39}Ar age data from the middle Latin valley volcanic field, Roman Magmatic Province, Central Italy. *Journal of Petrology*, *50*(7), 1327–1357. https://doi.org/10.1093/petrology/egp003

Casalini, M., Avanzinelli, R., Tommasini, S., Elliott, T., & Conticelli, S. (2019). Ce/Mo and molybdenum isotope systematics in subduction-related orogenic potassic magmas of Central-Southern Italy. *Geochemistry, Geophysics, Geosystems*, *20*(6), 2753–2768. https://doi.org/10.1029/2019GC008193

Chakraborty, S. (2010). Diffusion coefficients in olivine, wadsleyite, and ringwoodite. *Reviews in Mineralogy and Geochemistry*, *72*(1), 603–639. https://doi.org/10.2138/rmg.2010.72.13

Conticelli, S. (1998). The effects of crustal contamination on ultrapotassic magmas with lamproitic affinity: Mineralogical, geochemical and isotope data from the Torre Alfina lavas and xenoliths, Central Italy. *Chemical Geology*, *149*, 51–81. https://doi.org/10.1016/S0009-2541(98)00038-2

Conticelli, S., Avanzinelli, R., Ammannati, E., & Casalini, M. (2015). The role of carbon from recycled sediments in the origin of ultrapotassic igneous rocks in the Central Mediterranean. *Lithos*, *232*, 174–196. https://doi.org/10.1016/j.lithos.2015.07.002

Conticelli, S., Avanzinelli, R., Poli, G., Braschi, E., & Giordano, G. (2013). Shift from lamproite-like to leucititic rocks: Sr-Nd-Pb isotope data from the Monte Cimino volcanic complex vs. the Vico stratovolcano, Central Italy. *Chemical Geology*, *353*, 246–266. https://doi.org/10.1016/j.jvolgeores.2012.04.015

Conticelli, S., Avanzinelli, R., Marchionni, S., Tommasini, S., & Melluso, L. (2011). Sr-Nd-Pb isotopes from the Radicofani Volcano, Central Italy: Constraints on heterogeneities in a veined mantle responsible for the shift from ultrapotassic shoshonite to basaltic andesite magmas in a post-collisional setting. *Mineralogy Petrology*, *103*, 123–148. https://doi.org/10.1007/s00710-011-0161-y

Conticelli, S., D'Antonio, M., Pinarelli, L., & Civetta, L. (2002). Source contamination and mantle heterogeneity in the genesis of Italian potassic and ultrapotassic volcanic rocks: Sr-Nd-Pb isotope data from Roman Province and Southern Tuscany. *Mineralogy and Petrology*, *74*(2–4), 189–222. https://doi.org/10.1007/s007100200004

Conticelli, S., Guarnieri, L., Farinelli, A., Mattei, M., Avanzinelli, R., Bianchini, G., et al. (2009). Trace elements and Sr-Nd-Pb isotopes of K-rich, shoshonitic, and calc-alkaline magmatism of the Western Mediterranean region: Genesis of ultrapotassic to calc-alkaline magmatic associations in a post-collisional geodynamic setting. *Lithos*, *107*(1–2), 68–92. https://doi.org/10.1016/j.lithos.2008.07.016

Conticelli, S., Marchionni, S., Rosa, D., Giordano, G., Boari, E., & Avanzinelli, R. (2009). Shoshonite and sub-alkaline magmas from an Ultrapotassic Volcano: Sr-Nd-Pb isotope data on the Roccamonfina volcanic rocks, Roman Magmatic Province, Southern Italy. *Contributions to Mineralogy and Petrology*, *157*, 41–63. https://doi.org/10.1007/s00410-008-0319-8

Conticelli, S., Laurenzi, M. A., Giordano, G., Mattei, M., Avanzinelli, R., Melluso, L., et al. (2010). Leucite-bearing (kamafugitic/leucititic) and -free (lamproitic) ultrapotassic rocks and associated shoshonites from Italy: Constraints on petrogenesis and geodynamics. In M. Beltrando, A. Peccerillo, M. Mattei, S. Conticelli, & C. Doglioni (Eds.), *The Geology of Italy. Journal of Virtual explorer* (Vol. *36*). Paper n. 20. https://doi.org/10.3809/jvirtex.2009.00251

Conticelli, S., Melluso, L., Perini, G., Avanzinelli, R., & Boari, E. (2004). Petrologic, geochemical and isotopic characteristics of potassic and ultrapotassic magmatism in Central-Southern Italy: Inferences on its genesis and on the nature of mantle sources. *Periodico di Mineralogia*, *73*, 135–164.

Conticelli, S., & Peccerillo, A. (1990). Petrological significance of high-pressure ultramafic xenoliths from ultrapotassic rocks of Central Italy. *Lithos*, *24*(4), 305–322. https://doi.org/10.1016/0024-4937(89)90050-9

Conticelli, S., & Peccerillo, A. (1992). Petrology and geochemistry of potassic and ultrapotassic volcanism in Central Italy: Petrogenesis and interferences on the mantle source. *Lithos*, *28*(3–6), 221–240. https://doi.org/10.1016/0024-4937(92)90008-M

Dallai,, L., Bianchini,, G., Avanzinelli,, R., Gaeta,, M., Deloule,, E., Natali,, C., et al. (2022). Rhyolite melts at mantle depths reveal crustal recycling within the dynamic Earth. *Nature Communication*, *13*, Article number 7765 (2022).

Dallai, L., Bianchini, G., Avanzinelli, R., Natali, C., & Conticelli, S. (2019). Heavy oxygen recycled into the lithospheric mantle. *Scientific Reports*, *9*(1), 8793. https://doi.org/10.1038/s41598-019-45031-3

Danyushevsky, L., & Plechov, P. (2011). Petrolog3: Integrated software for modeling crystallization processes. *Geochemistry, Geophysics, Geosystems*, *12*(7). https://doi.org/10.1029/2011GC003516

Dasgupta, R., Hirschmann, M. M., & Smith, N. D. (2007). Partial melting experiments of peridotite + CO_2 at 3 Gpa and Genesis of Alkalic Ocean Island Basalts. *Journal of Petrology*, *48*(11), 2093–2124. https://doi.org/10.1093/petrology/egm053

De Hoog, J., Gall, L., & Cornell, D. (2010). Trace-element geochemistry of mantle olivine and application to mantle petrogenesis and geothermobarometry. *Chemical Geology*, *270*(1–4), 196–215. https://doi.org/10.1016/j.chemgeo.2009.11.017

Di Giuseppe, P., Agostini, S., Di Vincenzo, G., Manetti, P., Savaşçın, M. Y., & Conticelli, S. (2021). From subduction to strike slip-related volcanism: Insights from Sr, Nd, and Pb isotopes and geochronology of lavas from Sivas–Malatya region, Central Eastern Anatolia. *International Journal of Earth Sciences*, *110*(3), 849–874. https://doi.org/10.1007/s00531-021-01995-0

Di Rocco, T., Freda, C., Gaeta, M., Mollo, S., & Dallai, L. (2012). Magma chambers emplaced in carbonate substrate: Petrogenesis of skarn and cumulate rocks and implications for CO_2 degassing in volcanic areas. *Journal of Petrology*, *53*(11), 2307–2332. https://doi.org/10.1093/petrology/egs051

Di Stefano, F., Mollo, S., Scarlato, P., Nazzari, M., Bachmann, O., & Caruso, M. (2018). Olivine compositional changes in primitive magmatic skarn environments: A reassessment of divalent cation partitioning models to quantify the effect of carbonate assimilation. *Lithos*, *316–317*, 104–121. https://doi.org/10.1016/j.lithos.2018.07.008

Eiler, J. M. (2001). Oxygen isotope variations of basaltic lavas and upper mantle rocks. *Reviews in Mineralogy and Geochemistry*, *43*(1), 319–364. https://doi.org/10.2138/gsrmg.43.1.319

Eiler, J. M., Crawford, A., Elliot, T., Farley, K., Valley, J., & Stolper, E. (2000). Oxygen isotope geochemistry of oceanic-arc lavas. *Journal of Petrology*, *41*(2), 229–256. https://doi.org/10.1093/petrology/41.2.229

Facenna, C., Piromallo, C., Crespo-Blanc, L., Jolivet, L., & Rossetti, F. (2004). Lateral slab deformation and the origin of Western Mediterranean arcs. *Tectonics*, *23*(1), 1012. https://doi.org/10.1029/2002TC001488

Falloon, T. J., Danyushevsky, L. V., Ariskin, A., Green, D. H., & Ford, C. E. (2007). The application of olivine geothermometry to infer crystallization temperatures of parental liquids: Implications for the temperature of MORB magmas. *Chemical Geology*, *241*(3–4), 207–233. https://doi.org/10.1016/j.chemgeo.2007.01.015

Foley, S., & Peccerillo, A. (1992). Potassic and ultrapotassic magmas and their origin. *Lithos*, *28*(3–6), 181–185. https://doi.org/10.1016/0024-4937(92)90005-j

Foley, S., Prelević, D., Rehfeldt, T., & Jacob, D. (2013). Minor and trace elements in olivines as probes into early igneous and mantle melting processes. *Earth and Planetary Science Letters*, *363*, 181–191. https://doi.org/10.1016/j.epsl.2012.11.025

Foley, S., Venturelli, G., Green, D. H., & Toscani, L. (1987). The ultrapotassic rocks: Characteristics, classification, and constraints for petrogenetic models. *Earth-Science Reviews*, *24*(2), 81–134. https://doi.org/10.1016/0012-8252(87)90001-8

Foley, S. F. (1985). The oxidation state of lamproitic magmas. *Tschermaks Mineralogische und Petrographische Mitteilungen*, *34*(3–4), 217–238. https://doi.org/10.1007/bf01082963

Foley, S. F. (1992). Vein-plus-wall-rock melting mechanisms in the lithosphere and the origin of potassic alkaline magmas. *Lithos*, *28*(3–6), 435–453. https://doi.org/10.1016/0024-4937(92)90018-t

Förster, M. W., Buhre, S., Xu, B., Prelević, D., Mertz-Kraus, R., & Foley, S. F. (2020). Two-stage origin of K-enrichment in ultrapotassic magmatism simulated by melting of experimentally metasomatized mantle. *Minerals*, *10*(1), 41. https://doi.org/10.3390/min10010041

Förster, M. W., Prelević, D., Buhre, S., Mertz-Kraus, R., & Foley, S. F. (2019). An experimental study of the role of partial melts of sediments versus mantle melts in the sources of potassic magmatism. *Journal of Asian Earth Sciences*, *177*, 76–88. https://doi.org/10.1016/j.jseaes.2019.03.014

Gaeta, M., Di Rocco, T., & Freda, C. (2009). Carbonate assimilation in open magmatic systems: The role of melt-bearing skarns and cumulate forming processes. *Journal of Petrology*, *50*(2), 361–385. https://doi.org/10.1093/petrology/egp002

Gale, A., Dalton, C. A., Langmuir, C. H., Su, Y., & Schilling, J.-G. (2013). The mean composition of ocean ridge basalts. *Geochemistry, Geophysics, Geosystems*, *14*(3), 489–518. https://doi.org/10.1029/2012GC004334

Genske, F. S., Beier, C., Haase, K. M., Turner, S. P., Krumm, S., & Brandl, P. A. (2013). Oxygen isotopes in the Azores islands: Crustal assimilation recorded in olivine. *Geology*, *41*(4), 491–494. https://doi.org/10.1130/G33911.1

Grassi, D., & Schmidt, M. W. (2011). The melting of carbonated pelites from 70 to 700 km depth. *Journal of Petrology*, *52*(4), 765–789. https://doi.org/10.1093/petrology/egr002

Green, T. H., & Ringwood, A. E. (1968). Genesis of the calc-alkaline igneous rock suite. *Contributions to Mineralogy and Petrology*, *18*(2), 105–162. https://doi.org/10.1007/bf00371806

Griffin, W., Powell, W., Pearson, N. J., & O'Reilly, S. (2008). GLITTER: Data reduction software for laser ablation ICP-MS. In P. Sylvester (Ed.), *Laser Ablation ICP-MS in the Earth Sciences: Current practices and outstanding issues* (Vol. 40, pp. 307–311). Mineralogical Association of Canada, Short Course Series.

Gurenko, A. A., Bindemann, I. N., & Chaussidon, M. (2011). Oxygen isotope heterogeneity of the mantle beneath the Canary Islands: Insights from olivine phenocrysts. *Contributions to Mineralogy and Petrology*, *162*(2), 349–363. https://doi.org/10.1007/s00410-0100600-5

Gurenko, A. A., & Chaussidon, M. (2002). Oxygen isotope variations in primitive tholeiites of Iceland: Evidence from a SIMS study of glass inclusions, olivine phenocrysts and pillow rim glasses. *Earth and Planetary Science Letters*, *205*(1–2), 63–79. https://doi.org/10.1016/S0012-821X(02)01005-1

Hill, R., & Roeder, P. (1974). The crystallization of spinel from basaltic liquid as a function of oxygen fugacity. *The Journal of Geology*, *82*(6), 709–729. https://doi.org/10.1086/628026

Hirose, K. (1997). Melting experiments on lherzolite KLB-1 under hydrous conditions and generation of high-magnesian andesitic melts. *Geology*, *25*(1), 42–44. https://doi.org/10.1130/0091-7613(1997)025<0042:meolku>2.3.co;2

Hirose, K., & Kawamoto, T. (1995). Hydrous partial melting of lherzolite at 1 GPa: The effect of H_2O on the genesis of basaltic magmas. *Earth and Planetary Science Letters*, *133*(3–4), 463–473. https://doi.org/10.1016/0012-821x(95)00096-u

Hirose, K., & Kushiro, I. (1993). Partial melting of dry peridotites at high pressures: Determination of compositions of melts segregated from peridotite using aggregates of diamond. *Earth and Planetary Science Letters*, *114*(4), 477–489. https://doi.org/10.1016/0012-821x(93)90077-m

Hole, M. J. (1988). Post-subduction alkaline volcanism along the Antarctic Peninsula. *Journal of the Geological Society*, *145*(6), 985–998. https://doi.org/10.1144/gsjgs.145.6.0985

Howarth, G., & Harris, C. (2017). Discriminating between pyroxenite and peridotite sources for continental flood basalts (CFB) in Southern Africa using olivine chemistry. *Earth and Planetary Science Letters*, *475*, 143–151. https://doi.org/10.1016/j.epsl.2017.07.043

Iacono-Marziano, G., Gaillard, F., & Pichavant, M. (2007). Limestone assimilation and the origin of CO_2 emissions at the Alban Hills (Central Italy): Constraints from experimental petrology. *Journal of Volcanology and Geothermal Research*, *166*(2), 91–105. https://doi.org/10.1016/j.jvolgeores.2007.07.001

Iacono-Marziano, G., Gaillard, F., & Pichavant, M. (2008). Limestone assimilation by basaltic magmas: An experimental re-assessment and application to Italian volcanoes. *Contributions to Mineralogy and Petrology*, *155*(6), 719–738. https://doi.org/10.1007/s00410-007-0267-8

Jeffcoate, A. B., Elliott, T., Kasemann, S. A., Ionov, D., Cooper, K., & Brooker, R. (2007). Li isotope fractionation in peridotites and mafic melts. *Geochimica et Cosmochimica Acta*, *71*(1), 202–218. https://doi.org/10.1016/j.gca.2006.06.1611

Jochum, K., Nohl, U., Herwig, K., Lammel, E., Stoll, B., & Hofmann, A. (2007). GeoReM: A new geochemical database for reference materials and isotopic standards. *Geostandards and Geoanalytical Research*, *29*(3), 333–338. https://doi.org/10.1111/j.1751-908X.2005.tb00904.x

Jugo, P. J. (2009). Sulfur content at sulfide saturation in oxidized magmas. *Geology*, *37*(5), 415–418. https://doi.org/10.1130/g25527a.1

Kessel, R., Schmidt, M. W., Ulmer, P., & Pettke, T. (2005). Trace element signature of subduction-zone fluids, melts and supercritical liquids at 120-180 km depth. *Nature*, *437*(7059), 724–727. https://doi.org/10.1038/nature03971

Kokfelt, T., Hoernle, K., Hauff, F., Fiebig, J., Werner, R., & Garbe-Schönberg, D. (2006). Combined trace element and Pb-Nd-Sr-O isotope evidence for recycled oceanic crust (upper and lower) in the Iceland mantle plume. *Journal of Petrology*, *47*(9), 1705–1749. https://doi.org/10.1093/petrology/egl025

Le Bas, M. J., Le Maitre, R. W., Streckeisen, A., & Zanettin, B. A. (1986). Chemical classification of volcanic rocks based on the total alkali-silica diagram. *Journal of Petrology*, *27*, 745–750.

Lavecchia, G., & Stoppa, F. (1996). The tectonic significance of Italian magmatism: An alternative view to the popular interpretation. *Terra Nova*, *8*(5), 435–446. https://doi.org/10.1111/j.1365-3121.1996.tb00769.x

Lavecchia, G., Stoppa, F., & Creati, N. (2006). Carbonatites and kamafugites in Italy: Mantle-derived rocks that challenge subduction. *Annals of Geophysics*, *49*(1), 389–402.

Le Roux, V., Lee, C.-T. A., & Turner, S. J. (2010). Zn/Fe systematics in mafic and ultramafic systems: Implications for detecting major element heterogeneities in the Earth's mantle. *Geochimica et Cosmochimica Acta*, *74*(9), 2779–2796. https://doi.org/10.1016/j.gca.2010.02.004

Lustrino, M., Duggen, S., & Rosenberg, C. L. (2011). The Central-Western Mediterranean: Anomalous igneous activity in an anomalous collisional tectonic setting. *Earth-Science Reviews*, *104*(1–3), 1–40. https://doi.org/10.1016/j.earscirev.2010.08.002

Lustrino, M., Luciani, N., Stagno, V., Narzisi, S., Masotta, M., & Scarlato, P. (2022). Experimental evidence on the origin of Ca-rich carbonated melts formed by interaction between sedimentary limestones and mantle-derived ultrabasic magmas. *Geology*, *50*(4), 476–480. https://doi.org/10.1130/g49621.1

Lustrino, M., Ronca, S., Caracausi, A., Bordenca, C. V., Agostini, S., & Faraone, D. B. (2020). Strongly SiO_2-undersaturated, CaO-rich kamafugitic Pleistocene magmatism in Central Italy (San Venanzo volcanic complex) and the role of shallow depth limestone assimilation. *Earth-Science Reviews*, *208*, 103256. https://doi.org/10.1016/j.earscirev.2020.103256

Massonne, H.-J. (1992). Evidence for low-temperature ultrapotassic siliceous fluids in subduction zone environments from experiments in the system K_2O MgO Al_2O_3 SiO_2 H_2O (KMASH). *Lithos*, *28*(3–6), 421–434. https://doi.org/10.1016/0024-4937(92)90017-s

Mattey, D., Lowry, D., & Macpherson, C. (1994). Oxygen isotope composition of mantle peridotite. *Earth and Planetary Science Letters*, *128*(3–4), 231–241. https://doi.org/10.1016/0012-821X(94)90147-3

Mischel, S., Mertz-Kraus, R., Jochum, K., & Scholz, D. (2017). TERMITE-An R script for fast reduction of LA-ICPMS data and its application to trace element measurements. *Rapid Communications in Mass Spectrometry*, *31*(13), 1079–1087. https://doi.org/10.1002/rcm.7895

Mitchell, R. H., & Bergman, S. C. (1991). *Petrology of lamproites*. Plenum Press.

Molli, G. (2008). Northern Apennine-Corsica orogenic system: An updated overview. In S. Siegesmund, B. Fugenschuh, & N. Froitzheim (Eds.), *Tectonic aspects of the Alpine-Dinaride-Carpathian System* (Vol. 298, pp. 413–442). Geological Society, London, Special Publication.

Neumann, E.-R., Wulff-Pedersen, E., Pearson, N. J., & Spencer, E. A. (2002). Mantle xenoliths from Tenerife (Canary Islands): Evidence for reactions between mantle peridotites and silicic carbonatite melts inducing Ca metasomatism. *Journal of Petrology*, *43*(5), 825–857. https://doi.org/10.1093/petrology/43.5.825

Nikogosian, I., Ersoy, Ö., Whitehouse, M., Mason, P. R. D., De Hoog, J., Wortel, M., & Van Bergen, M. (2016). Multiple subduction imprints in the mantle below Italy detected in a single lava flow. *Earth and Planetary Science Letters*, *449*, 12–19. https://doi.org/10.1016/j.epsl.2016.05.033

Pack, A., & Herwartz, D. (2014). The triple oxygen isotope composition of the Earth mantle and understanding variations in terrestrial rocks and minerals. *Earth and Planetary Science Letters*, *390*, 138–145. https://doi.org/10.1016/j.epsl.2014.01.017

Panina, L., Stoppa, F., & Usol'tseva, L. M. (2003). Genesis of melilitite rocks of Pian di Celle volcano, mbrian kamafugite province, Italy: Evidence from melt inclusions in minerals. *Petrology*, *11*, 365–382.

Patacca, E., Scandone, P., Di Luzio, E., Cavinato, G. P., & Parotto, M. (2008). Structural architecture of the central Apennines: Interpretation of the CROP 11 seismic profile from the Adriatic coast to the orographic divide. *Tectonics*, *27*(3), TC3006. https://doi.org/10.1029/2005TC001917

Peccerillo, A. (1998). Relationships between ultrapotassic and carbonate-rich volcanic rocks in Central Italy: Petrogenetic and geodynamic implications. *Lithos*, *43*(4), 267–279. https://doi.org/10.1016/s0024-4937(98)00016-4

Peccerillo, A. (2005). *Plio-quaternary volcanism in Italy: Petrology, geochemistry, geodynamics*. Springer.

Peccerillo, A. (2017). *Cenozoic volcanism in the Tyrrhenian Sea region* (p. 399). Springer.

Perini, G., & Conticelli, S. (2002). Crystallization conditions of Leucite-Bearing magmas and their implications on the magmatological evolution of ultrapotassic magmas: The Vico Volcano, Central Italy. *Mineralogy and Petrology*, *74*(2–4), 253–276. https://doi.org/10.1007/s007100200005

Plechov, P., Nikolai, N., Shcherbakov, V., & Tikhonova, M. (2017). Extreme-Mg olivines from venancite lavas of Pian di Celle Volcano (Italy). *Doklady Earth Sciences*, *474*(1), 507–510. https://doi.org/10.1134/S1028334X17050245

Poli, S. (2015). Carbon mobilized at shallow depths in subduction zones by carbonatitic liquids. *Nature Geoscience*, *8*, 633–636. https://doi.org/10.1038/NGEO2464

Prelević, D., & Foley, S. F. (2007). Accretion of arc-oceanic lithospheric mantle in the Mediterranean: Evidence from extremely high-Mg olivines and Cr-rich spinel inclusions from lamproites. *Earth and Planetary Science Letters*, *256*(1–2), 120–135. https://doi.org/10.1016/j.epsl.2007.01.018

Prelević, D., Foley, S. F., Romer, R., & Conticelli, S. (2008). Mediterranean Tertiary lamproites derived from multiple source components in postcollisional geodynamics. *Geochimica et Cosmochimica Acta*, *72*(8), 2125–2156. https://doi.org/10.1016/j.gca.2008.01.029

Prelević, D., Foley, S. F., Romer, R. L., Cvetković, V., & Downes, H. (2005). Tertiary ultrapotassic volcanism in Serbia: Constraints on petrogenesis and mantle source characteristics. *Journal of Petrology*, *46*(7), 1443–1487. https://doi.org/10.1093/petrology/egi022

Prelević, D., Jacob, D., & Foley, S. F. (2013). Recycling plus: A new recipe for the formation of Alpine-Himalayan orogenic mantle lithosphere. *Earth and Planetary Science Letters*, *362*, 187–197. https://doi.org/10.1016/j.epsl.2012.11.035

Putirka, K. D. (2005). Mantle potential temperatures at Hawaii, Iceland, and the mid-ocean ridge system, as inferred from olivine phenocrysts: Evidence for thermally driven mantle plumes. *Geochemistry, Geophysics, Geosystems*, *6*(5). https://doi.org/10.1029/2005GC000915

Putirka, K. D., Perfit, M., Ryerson, F. J., & Jackson, M. G. (2007). Ambient and excess mantle temperatures, olivine thermometry, and active vs. passive upwelling. *Chemical Geology*, *241*(3–4), 177–206. https://doi.org/10.1016/j.chemgeo.2007.01.014

Rehfeldt, T., Foley, S. F., Jacob, D. E., Carlson, R. W., & Lowry, D. (2008). Contrasting types of metasomatism in dunite, wehrlite and websterite xenoliths from Kimberley, South Africa. *Geochimica et Cosmochimica Acta*, *72*(23), 5722–5756. https://doi.org/10.1016/j.gca.2008.08.020

Rehfeldt, T., Jacob, D. E., Carlson, R. W., & Foley, S. F. (2007). Fe-Rich dunite xenoliths from South African kimberlites:cumulates from Karoo flood basalts. *Journal of Petrology*, *48*(7), 1387–1409. https://doi.org/10.1093/petrology/egm023

Rittmann, A. (1933). Die geologische bedingte evolution und differentiation des Somma-Vesuvius magmas. *Zeitschrift für Vulkanologie*, *15*, 8–94.

Rosatelli, G., Stoppa, F., & Jones, A. P. (2000). Intrusive calcio-carbonatite occurrence from Mt. Vulture Volcano, Southern Italy. *Mineralogical Magazine*, *64*(4), 615–624. https://doi.org/10.1180/002646100549643

Scambelluri, M., & Philippot, P. (2001). Deep fluids in subduction zones. *Lithos*, *55*(1–4), 213–227. https://doi.org/10.1016/s0024-4937(00)00046-3

Sharygin, V., Pospelova, L., Smirnov, S., & Vladykin, N. (2003). Ni-rich sulfide inclusions in early lamproite minerals. *Geologiya I Geofizika*, *44*, 855–856.

Sekine, T., & Wyllie, P. J. (1982). Phase Relationships in the system $KAlSiO_4$-Mg_2SiO_4-SiO_2-H_2O as a model for hybridization between hydrous siliceous melts and peridotite. *Contributions to Mineralogy and Petrology*, *79*(4), 368–374. https://doi.org/10.1007/bf01132066

Smythe, D. J., Wood, B. J., & Kiseeva, E. S. (2017). The S content of silicate melts at sulfide saturation: New experiemnts and a model incorporating the effects of sulfide composition. *American Mineralogist*, *102*(4), 795–803. https://doi.org/10.2138/am-2017-5800ccby

Sobolev, A., Hofmann, A., Kuzmin, D., Yaxley, G., Arndt, N., Chung, S.-L., et al. (2007). The amount of recycled crust in sources of mantle-derived melts. *Science*, *316*(5823), 412–417. https://doi.org/10.1126/science.1138113

Sobolev, A., Hofmann, A., Sobolev, S. V., & Nikogosian, I. K. (2005). An olivine free mantle source of Hawaiian shield basalts. *Nature*, *434*(7033), 590–597. https://doi.org/10.1038/nature03411

Sokol, K., Prelević, D., Romer, R. L., Božović, M., van den Bogaard, P., Stefanova, E., et al. (2020). Cretaceous ultrapotassic magmatism from the Sava-Vardar zone of the Balkans. *Lithos*, *354–355*, 105268. https://doi.org/10.1016/j.lithos.2019.105268

Stoppa, F. (1996). The San Venanzo maar and tuff ring, Umbria, Italy: Eruptive behavior of a carbonatite-melilitite volcano. *Bulletin of Volcanology*, *57*(7), 563–577. https://doi.org/10.1007/BF00304440

Stoppa, F. (2003). Consensus and open questions about Italian CO_2—driven magma from the mantle. *Periodico di Mineralogia*, *72*(1), 1–8.

Stoppa, F., & Cundari, A. (1998). Origin and multiple crystallization of the kamafugite-carbonatite association: The San Venanzo-Pian di Celle occurrence (Umbria, Italy). *Mineralogical Magazine*, *62*(2), 273–289. https://doi.org/10.1180/002646198547530

Straub, S., La Gatta, A. B., Martin-Del Pozzo, A. L., & Langmuir, C. H. (2008). Evidence from high-Ni olivines for a hybridized peridotite/pyroxenite source for orogenic andesites from the central Mexican Volcanic Belt. *Geochemistry, Geophysics, Geosystems*, *9*(3), Q03007. https://doi.org/10.1029/2007gc001583

Tatsumi, Y., & Kogiso, T. (1997). Trace element transport during dehydration processes in the subducted oceanic curst: 2. Origin of chemical and physical characteristics in arc magmatism. *Earth and Planetary Science Letters*, *148*(1–2), 207–221. https://doi.org/10.1016/s0012-821x(97)00019-8

Thirlwall, M. F., Gee, M. A., Taylor, R. N., & Murton, B. J. (2004). Mantle components in Iceland and adjacent ridges investigated using double-spike Pb isotope ratios. *Geochimica et Cosmochimica Acta*, *68*(2), 361–386. https://doi.org/10.1016/s0016-7037(03)00424-1

Thomsen, T. B., & Schmidt, M. W. (2008). Melting of carbonated pelites at 2.5–5.0 GPa, silicate–carbonatite liquid immiscibility, and potassium–carbon metasomatism of the mantle. *Earth and Planetary Science Letters*, *267*(1–2), 17–31. https://doi.org/10.1016/j.epsl.2007.11.027

Turi, B. (1970). Carbon and oxygen isotopic composition of carbonates in limestone blocks and related geodes from the "Black Pozzolans" formation of the Alban Hills. *Chemical Geology*, *5*(3), 195–205. https://doi.org/10.1016/0009-2541(70)90052-5

Wenzell, T., Baumgartner, L. P., Brügmann, G. E., Konnikov, E. G., & Kislov, E. V. (2002). Partial melting and assimilation of dolomitic xenoliths by mafic magma: The Ioko–Dovyren intrusion (north Baikal region, Russia). *Journal of Petrology*, *43*(11), 2049–2074. https://doi.org/10.1093/petrology/43.11.2049

Wenzell, T., Baumgartner, L. P., Brügmann, G. E., Konnikov, E. G., Kislov, E. V., & Orsoev, D. A. (2001). Contamination of mafic magma by partial melting of dolomitic xenoliths. *Terra Nova*, *13*(3), 197–202. https://doi.org/10.1046/j.1365-3121.2001.00340.x

Wyllie, P. J., & Sekine, T. (1982). The formation of mantle phlogopite in subduction zone hybridization. *Contributions to Mineralogy and Petrology*, *79*(4), 375–380. https://doi.org/10.1007/bf01132067

Yoder, H. S., & Tilley, C. E. (1962). Origin of basalt magmas. *Journal of Petrology*, *3*, 343–532. https://doi.org/10.1093/petrology/3.3.342

Zanon, V. (2005). Geology and volcanology of San Venanzo volcanic field (Umbria, Central Italy). *Geological Magazine*, *142*(6), 683–698. https://doi.org/10.1017/Soo16756805001470

Zellmer, G. F., Freymuth, H., Cembrano, J. M., Clavero, E., Veloso, E. A., & Sielfeld, G. (2013). *Altered mineral uptake into fresh arc magmas: Insights from U–Th isotopes of samples from Andean volcanoes under differential crustal stress regimes* (Vol. 385). Geological Society. Special Publications. https://doi.org/10.1144/SP385.9

Zellmer, G. F., Sakamoto, N., Iizuka, Y., Miyoshi, M., Tamura, Y., Hsieh, H.-H., & Yurimoto, H. (2014). Crystal uptake into aphyric arc melts: Insights from two-pyroxene pseudo-decompression paths, plagioclase hygrometry, and measurement of hydrogen in olivines from mafic volcanics of SW Japan. *Geological Society, London, Special Publications*, *385*(1), 161–184. https://doi.org/10.1144/SP385.3